Supporting Information

Regulating alternative lifestyles in entomopathogenic bacteria

Jason M. Crawford[*], Renee Kontnik[*], and Jon Clardy[†]

***** These authors contributed equally to this work.
† To whom correspondence may be addressed.

Department of Biological Chemistry & Molecular Pharmacology, Harvard Medical School, 240 Longwood Avenue, Boston, MA 02115.

List of Supporting Information

Bacterial lifestyle and proline utilization

Photorhabdus and *Xenorhabdus* species are in the antibiotic producing, primary form during insect infection, in which they exhibit higher titers of antibacterial, antifungal, and insecticidal activities [1-3]. For reasons not understood, it was previously noted that the primary and secondary forms that occur in stationary phase of *Photorhabdus* and *Xenorhabdus* display differences in respiratory enzyme activity, proline uptake, and PMF depending on their growth conditions [4]. The secondary form exhibits significantly reduced lag phases and five-fold greater proline uptake compared to the primary form. It was therefore proposed that the secondary form was more adapted to living independently in the soil, but neither *Photorhabdus* nor *Xenorhabdus* isolates have been observed outside of their mutualistic nematode hosts. Analyses of the *P. luminescens-Heterorhabditis* pair have demonstrated that the nematode is capable of carrying both forms of the bacteria, and a mixture of the two can be recovered from infective juveniles [5, 6], although the primary form is favored. Moreover, both forms are equally virulent to insect larvae [7]. We could therefore envision a scenario where a variable mixture of primary and secondary forms could be dispatched into the insect, the former to expedite production of antimicrobials and molecules critical for nematode symbiosis, and the latter to accelerate population density early in the infection process. The evolutionary conservation of both forms could in this way provide the ultimate competitive fitness.

Supporting Materials and Methods

Metabolite stimulation. *P. luminescens* and *X. nematophila* suspension cultures (5 mL: 2 g/L tryptone, 5 g/L yeast-extract, and 10 g/L NaCl as the base medium plus additional stated supplements unless otherwise indicated) were grown to stationary phase over 72 hours at 30 ºC and 250 rpm (Fig. S2). The cultures were vigorously extracted with 6 mL of ethyl acetate, centrifuged, and 4 mL of the top organic layer was dried for analysis. The dried ethyl acetate extracts of *P. luminescens* and *X. nematophila* were resuspended in 1 mL and 0.5 mL methanol, respectively. 50 μL of this mixture was injected for HPLC analysis in order to quantify metabolite production. Separation was performed over a Discovery RP-amide C16 (25 cm x 4.6 mm, 5 μM, Supelco) HPLC column with an acetonitrile:water gradient at 1mL/min. Method for *P. luminescens* extracts: 0-2 min, 10 % MeCN; 2-10 min, 10-50% MeCN; 10-25 min, 50-75% MeCN. Method for *X. nematophila* extracts: 0-2 min, 10% MeCN; 2-20 min, 10-40% MeCN; 20-35 min; 40-100% MeCN. All metabolite stimulation experiments were performed in triplicate.

Induction factor identification. *G. mellonella* larvae were frozen in liquid nitrogen and ground to a fine powder. The powder was extracted with organic and aqueous solvents, but only the aqueous extracts exhibited activity. Hemolymph similarly exhibited activity.

Hemolymph was then collected from 500 *G. mellonella* larvae. Fresh hemolymph stored on ice was diluted with 100 mM potassium phosphate buffer (pH = 7.4) and filtered through a 3,000 molecular weight cutoff membrane (Amicon Ultra, Millipore); the activity resided in the flow through. The Amicon filter flow through of diluted *G. mellonella* hemolymph was concentrated and separated over a Discovery RP-amide C16 (25 cm x 10 mm, 5 μM, Supelco) HPLC column with an acetonitrile:water gradient at 2mL/min: 0-10 min, 2% MeCN; 10-40 min, 2-100% MeCN. Fractions were collected in 1-minute intervals, concentrated, and added to *P. luminescens* and *X. nematophila* cultures. Activity was

found to elute at 7 min, in the initial isocratic step. This fraction was further purified on a HYPERCARB (100 x 4.6 mm, 5 μM, Thermo Scientific) column: 0.5 mL/min; 0-10 min, 0% MeCN; 10-15 min, 0-50% MeCN. Activity eluted in the fraction at 3 minutes. NMR analysis of this fraction revealed the active factor to be proline (Fig. S1). Subsequent two-dimensional NMR analyses (COSY, HSQC, and HMBC) were consistent with proline (data not shown). Bacterial metabolite stimulation was confirmed by the addition of commercially available L-proline (Fig. 3). D-proline exhibited little effect compared to control cultures lacking proline (Fig. S2). Metabolite stimulation by L-proline was physiologically relevant as demonstrated by complete amino acid analysis on selected host insect larvae (Table S1).

Allelic-exchange mutagenesis. Using the highly similar *E. coli* proteins as bioinformatics probes (blastp) against the published sequence of *P. luminescens* TT01 [8], we identified two *P. luminescens* homologs, PutP (local alignment, *id/sim/gap*, 77.0/87.7/0.0) and ProU (ProU consists of three proteins: ProV, 73.1/86.4/0.0; ProX, 71.6/84.5/0.0; and ProW, 72.5/84.4/3.1), for proline transport. *P. luminescens putP* and *proU* genes were excised from the genome by allelic exchange mutagenesis for further interrogation.

P. luminescens gDNA was isolated using previously described procedures [9]. The entire coding sequence (from start to stop codons) of *putP* was excised by allelic-exchange mutagenesis. The exchange sequence for *putP* consisted of ~1 kB of upstream and downstream genome sequence fused by overlap extension PCR [10]. The first fragment was amplified with primer pairs PutP-A5 and PutP-A3, and the second fragment was amplified with primer pairs PutP-B5 and PutP-B3 (Table S7). The two products were used as templates in the final PCR, using primer pairs PutP-A5 and PutP-B3, thereby fusing the two pieces. The full-length *putP* exchange sequence was digested with SacI, inserted into the corresponding site in pDS132 [11], and verified by restriction analysis (pDΔPutP). Cloning was carried out in *E. coli* strain WM3618 lambda pir. pDS132 has been used successfully for allelic-exchange in *P. luminescens* [12].

The *proU* deletion (*proV*, *proW*, and *proX*) construct was constructed similarly to the *putP* deletion construct. The first fragment was amplified with primer pairs ProU-A5 and ProU-A3, and the second fragment was amplified with primer pairs ProU-B5 and ProU-B3. The exchange sequence was amplified using ProU-A5 and ProU-B3 to generate the full-length DNA piece. The sequence was digested with SphI, inserted into the corresponding site in pDS132, and verified by restriction analysis (pDΔProU).

The pDS132 deletion constructs (pDΔPutP or pDΔProU) were transformed into the diaminopimelic acid (dap) auxotroph donor strain, *E. coli* WM6026 lambda pir [13], by heat-shock transformation [14]. The donor *E. coli* and recipient *P. luminescens* were grown to OD_{600} = 0.6-0.8, mixed in a 1:1 ratio, filtered through a 0.2 μM sterile filter, and allowed to filter mate on LB agar supplemented with 0.3 mM dap overnight at 30 °C.

The mating mixture was resuspended in liquid LB and plated on LB chloramphenicol (50 μg/mL) plates lacking supplemental dap. *P. luminescens* colonies identified by their yellow color phenotype were re-plated on LB with chloramphenicol and grown at 30 °C. Single colonies were then streaked onto LB sucrose (5%) plates for SacB counter selection. Single colonies growing on sucrose plates were subjected to colony PCR using primer pairs PutP5-genome and PutP3-genome or ProU5-genome

and ProU3-genome to identify successful deletion mutants. The mutants were re-streaked three times on LB from single colonies and reanalyzed by colony PCR. The PCR products from successful deletion mutants were sequence verified.

Phenotypic growth effects. *P. luminescens* and *X. nematophila* single colonies were selected and grown for two days in LB at 30 °C. 30 μL of the suspensions were streaked onto agar plates (salt experiments: 2 g tryptone, 5 g yeast-extract, and 0, 10, or 35 g NaCl per L agar; sorbitol experiment: 2 g tryptone and 5 g yeast-extract per L agar, with 750 mM sorbitol) containing bromothymol blue and TTC and grown for 3-5 days at 30 °C [5]. These experiments were conducted with and without 100 mM L-proline and/or 10 uM CCCP. The results of these experiments are presented in Figures S8-S16.

NMR analysis. NMR experiments (Varian: ^{1}H, gCOSY, gHSQC, gHMBC, and ROESY) were performed in deuterated methanol, water, dimethyl sulfoxide, or chloroform with a symmetrical NMR microtube susceptibility-matched with the appropriate solvent (Shigemi, Inc.) on a Varian INOVA 600 MHz NMR. Known metabolites were confirmed by ^{1}H NMR and mass spectrometry. ^{1}H and ^{13}C data (Tables S3-S6), high-resolution MS data (Table S2), and 2D-NMR spectra (Figs. S19-S31) are shown for **1**, **7**, and **8**.

HPLC peaks corresponding to metabolites upregulated by hemolymph or L-proline were collected and purified further if necessary. Spectral analysis of the three selected *P. luminescens* metabolites by mass spectrometry and ^{1}H NMR showed them to be identical to the previously reported anthraquinone **2** and stilbenes **3** and **4** [15, 16]. In *X. nematophila*, indole-containing metabolites were similarly verified as nematophin (**5**) [17], its reduction product (**6**) [18-20], and xenamatide (**9**) [21]. Polarimetry measurements, $[\alpha]_D$ = -24.0, c = .13, MeOH, support stereochemical assignments of **6**.

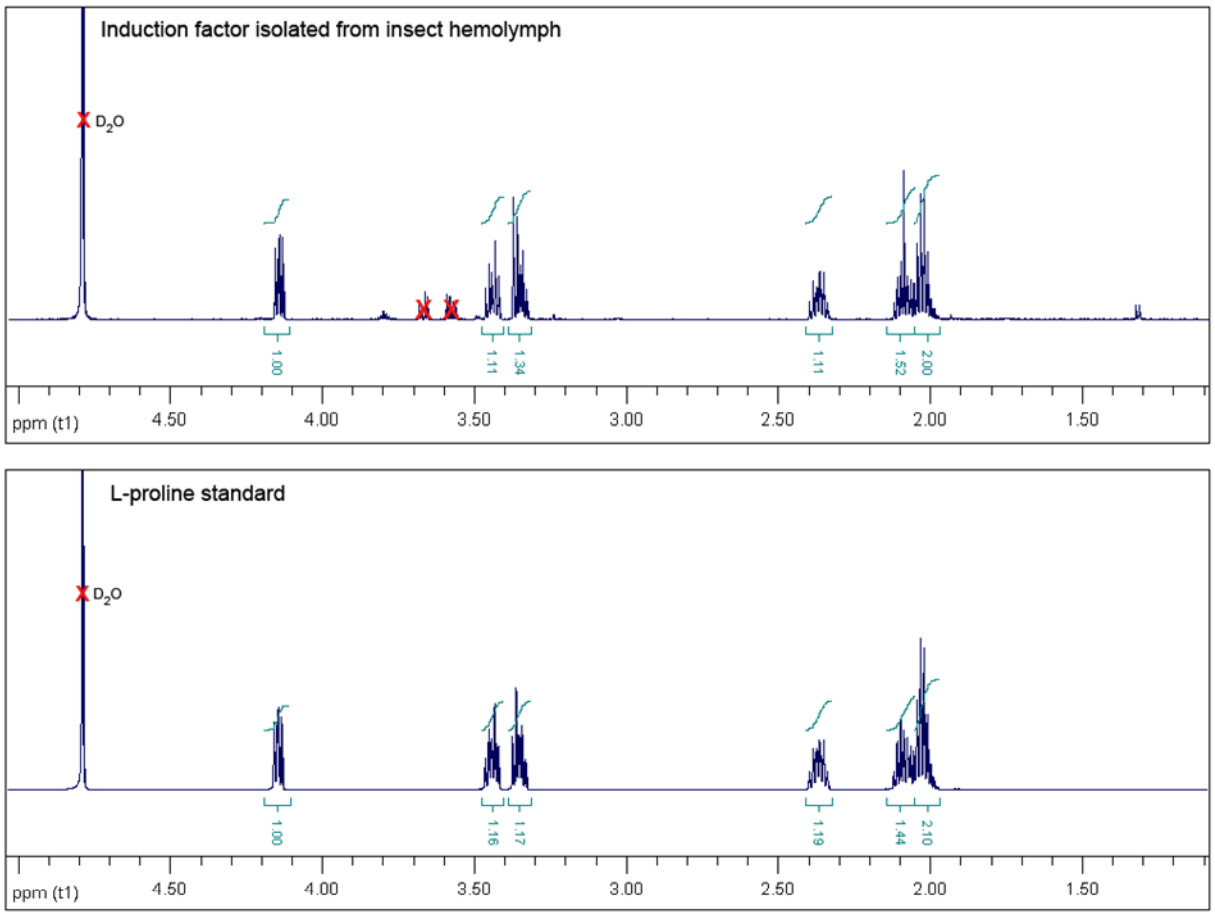

Figure S1. NMR of purified induction factor. ^{1}H NMR analysis of the purified bacterial metabolite induction factor (top) from insect hemolymph matched that of L-proline (bottom). Red X's indicate either solvent (D_2O) or minor contaminant (top). Subsequent LC/MS analysis (M-H = 114.1) and two-dimensional NMR analyses (COSY, HSQC, and HMBC) of the induction factor were also consistent with proline (data not shown).

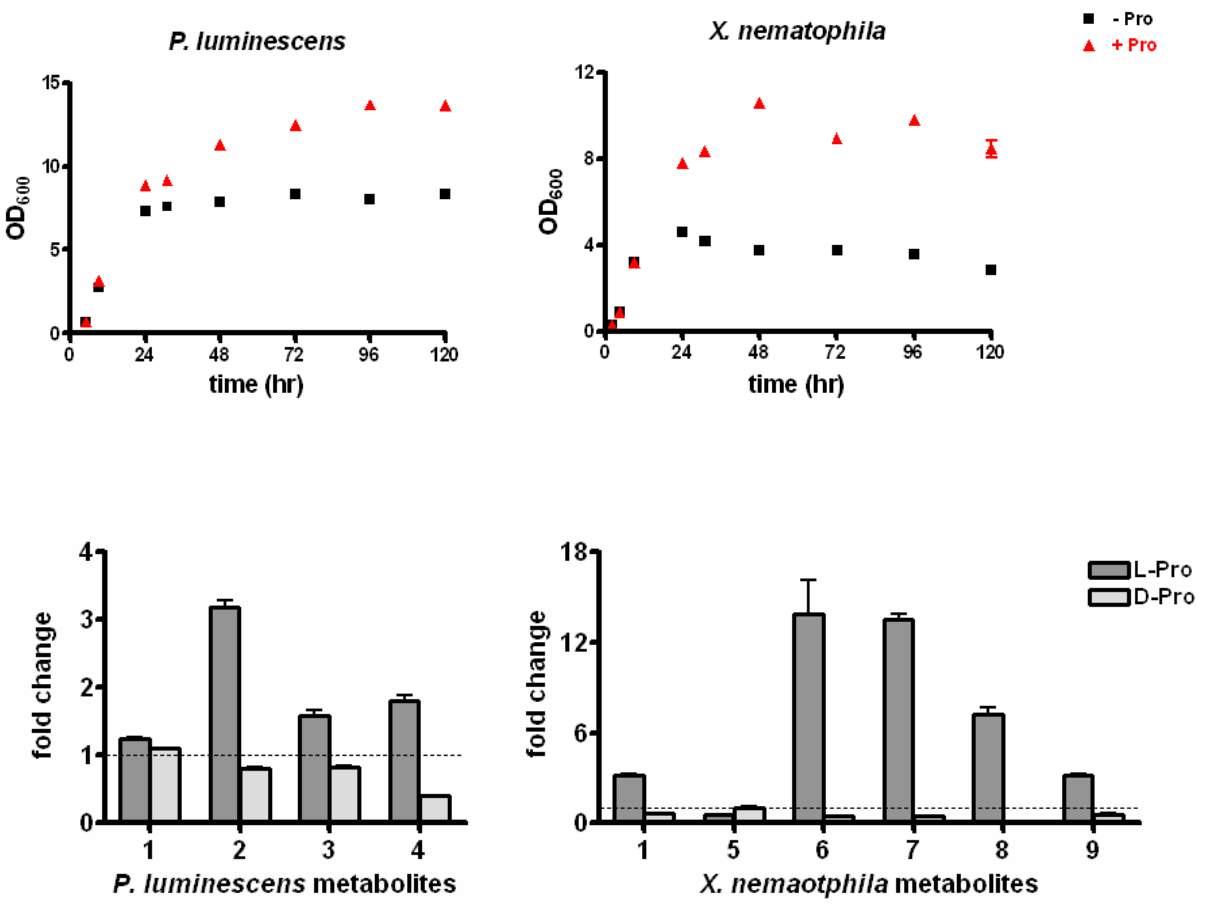

Figure S2. Growth curves of *P. luminescens* and *X. nematophila* and induction with L- vs. D-proline. Top: Cell densities (OD_{600}) of *P. luminescens* (left) and *X. nematophila* (right) cultures were measured over a 120-hour time course. A 72-hour time point was chosen for metabolite analyses in all experiments, after bacteria had reached stationary phase. Cultures were grown in a rich tryptone-yeast extract based medium (2 g tryptone, 5 g yeast extract, and 10 g NaCl per L) with and without 50 mM L-proline. **Bottom:** Supplementation of the culture medium with L-proline, but not D-proline, led to upregulation of most bacterial metabolites (50 mM L- or D-proline supplementation to the tryptone-yeast extract based medium). The dashed line represents metabolite production in control cultures without L- or D-proline supplementation (error bars = s.d. (+/-)). Numbers on the *x*-axis represent metabolites illustrated in Fig 1. Rhabduscin (**1**) production in *P. luminescens* (left) was not affected by proline, but was regulated by osmolarity in our studies (Fig. S5). The majority of the *X. nematophila* (right) metabolites were upregulated with L-proline. Nematophin (**5**) decreased in L-proline supplemented cultures, as in hemolymph supplemented cultures (Fig. 2), in keeping with the observed metabolic shift.

Table S1. Free amino acid concentrations in insect hemolymph and media control. (All concentrations in mM.)

Galleria mellonella

	1	2	3	Avg.	Std.dev.
Ala	27.0	29.8	32.4	**29.8**	2.7
Arg	5.15	6.97	6.60	**6.24**	1.0
Asn	4.95	5.20	6.99	**5.71**	1.1
Asp	0.47	0.53	0.51	**0.50**	0.0
Cys	0.41	0.42	0.40	**0.41**	0.0
Glu	0.00	0.00	0.00	**0.00**	0.0
Gln	94.8	98.6	106.0	**99.8**	5.7
Gly	16.8	20.8	26.1	**21.2**	4.6
His	9.00	8.96	0.00	**5.98**	5.2
Ile	3.39	3.61	4.17	**3.72**	0.4
Leu	4.57	4.89	5.92	**5.13**	0.7
Lys	6.79	7.04	6.18	**6.67**	0.4
Met	0.85	0.71	1.11	**0.89**	0.2
Phe	1.39	1.67	1.86	**1.64**	0.2
Pro	64.2	79.0	74.7	**72.6**	7.6
Ser	6.79	7.27	10.2	**8.07**	1.8
Thr	4.69	4.52	4.94	**4.72**	0.2
Trp	0.00	0.00	0.00	**0.00**	0.0
Tyr	1.06	1.06	0.00	**0.71**	0.6
Val	6.44	6.92	8.64	**7.33**	1.2

Zophobus morio

	1	2	3	Avg.	Std.dev.
Ala	4.71	5.68	7.32	**5.90**	1.3
Arg	3.79	3.27	3.76	**3.60**	0.3
Asn	0.00	2.96	0.55	**1.17**	1.6
Asp	0.00	0.74	1.02	**0.59**	0.5
Cys	0.42	0.38	0.44	**0.41**	0.0
Glu	0.20	1.92	2.91	**1.67**	1.4
Gln	31.6	18.5	38.4	**29.5**	10.1
Gly	2.46	2.16	2.57	**2.39**	0.2
His	9.14	9.76	9.54	**9.48**	0.3
Ile	3.07	2.08	2.58	**2.58**	0.5
Leu	1.65	2.20	3.14	**2.33**	0.8
Lys	12.2	12.8	10.8	**11.9**	1.1
Met	0.80	0.19	0.23	**0.40**	0.3
Phe	0.69	1.47	1.70	**1.29**	0.5
Pro	63.0	54.6	59.4	**59.0**	4.2
Ser	3.09	3.19	4.60	**3.62**	0.8
Thr	0.75	1.40	1.69	**1.28**	0.5
Trp	0.00	1.21	2.87	**1.36**	1.4
Tyr	1.64	2.29	2.40	**2.11**	0.4
Val	4.40	4.37	5.80	**4.85**	0.8

Tenebrio molitor

	1	2	3	Avg.	Std.dev.
Ala	6.27	4.85	3.90	**5.01**	1.2
Arg	2.89	2.44	1.89	**2.41**	0.5
Asn	0.00	0.00	0.00	**0.00**	0.0
Asp	2.96	1.91	1.77	**2.21**	0.7
Cys	0.61	0.54	0.55	**0.57**	0.0
Glu	11.6	9.25	8.50	**9.78**	1.6
Gln	0.00	0.00	0.00	**0.00**	0.0
Gly	6.21	4.78	4.72	**5.23**	0.8
His	7.19	6.19	6.39	**6.59**	0.5
Ile	5.00	4.01	3.70	**4.24**	0.7
Leu	7.21	5.40	5.09	**5.90**	1.1
Lys	10.7	9.03	9.13	**9.63**	1.0
Met	1.40	1.14	0.99	**1.17**	0.2
Phe	2.17	1.68	1.65	**1.83**	0.3
Pro	34.8	28.7	28.9	**30.8**	3.5
Ser	4.86	4.27	4.30	**4.47**	0.3
Thr	3.50	2.79	2.66	**2.98**	0.5
Trp	0.00	0.00	0.90	**0.30**	0.5
Tyr	2.32	1.52	1.38	**1.74**	0.5
Val	9.43	6.99	6.67	**7.70**	1.5

Manduca sexta

	1	2	3	Avg.	Std.dev.
Ala	2.37	1.82	2.42	**2.20**	0.3
Arg	7.02	5.26	7.63	**6.63**	1.2
Asn	1.60	2.62	3.27	**2.50**	0.8
Asp	0.13	0.00	0.14	**0.09**	0.1
Cys	0.44	0.45	0.44	**0.44**	0.0
Glu	0.68	0.00	0.85	**0.51**	0.4
Gln	10.1	13.6	13.1	**12.3**	1.9
Gly	22.5	26.2	16.8	**21.8**	4.8
His	11.3	11.8	10.5	**11.2**	0.6
Ile	1.53	1.35	1.77	**1.55**	0.2
Leu	1.31	1.23	1.89	**1.48**	0.4
Lys	4.59	5.03	5.12	**4.91**	0.3
Met	1.21	0.86	0.96	**1.01**	0.2
Phe	0.36	0.27	0.72	**0.45**	0.2
Pro	3.43	2.48	4.48	**3.46**	1.0
Ser	9.26	9.65	7.23	**8.71**	1.3
Thr	3.12	2.60	2.96	**2.89**	0.3
Trp	0.00	0.43	0.00	**0.14**	0.2
Tyr	0.00	0.00	1.63	**0.54**	0.9
Val	1.56	1.43	2.74	**1.91**	0.7

Media control

	1	2	3	Avg.	Std.dev.
Ala	2.34	3.03	3.38	**2.92**	0.53
Arg	0.61	0.79	0.91	**0.77**	0.15
Asn	0.00	0.00	0.00	**0.00**	0.00
Asp	0.71	0.91	1.01	**0.88**	0.15
Cys	0.40	0.47	0.39	**0.42**	0.04
Glu	2.31	3.01	3.43	**2.92**	0.57
Gln	0.00	0.00	0.00	**0.00**	0.00
Gly	0.73	0.92	1.00	**0.88**	0.14
His	0.00	0.00	0.20	**0.07**	0.11
Ile	0.94	2.02	1.30	**1.42**	0.55
Leu	1.75	2.61	2.56	**2.30**	0.48
Lys	0.89	1.07	1.32	**1.09**	0.22
Met	0.75	1.58	0.78	**1.04**	0.47
Phe	0.73	0.93	1.12	**0.92**	0.20
Pro	0.00	0.00	0.00	**0.00**	0.00
Ser	0.97	1.22	1.37	**1.18**	0.20
Thr	0.78	0.99	1.11	**0.96**	0.17
Trp	0.00	0.00	0.00	**0.00**	0.00
Tyr	0.00	0.20	0.24	**0.15**	0.13
Val	1.10	1.46	1.67	**1.41**	0.29

Table S1. Free amino acid concentrations in insect hemolymph. Complete amino acid analysis was conducted on hemolymph samples from four representative host insect larvae – *G. mellonella* (greater waxmoth), *Manduca sexta* (tobacco hornworm), *Tenebrio molitor* (mealworm), and *Zophobus morio* (superworm) – for the 20 proteinogenic amino acids. Insect larvae were obtained from Berkshire Biological. Hemolymph, which carries nutrients as insects respire by diffusion, has high free amino acid, carbohydrate, and inorganic salt concentrations, although these can vary substantially based on osmotic pressure, diet, and insect species [22]. While hemolymph L-proline concentrations have a substantial range (~20 fold), these findings show that the low mM L-proline concentrations needed to regulate metabolite production are physiologically relevant.

Metabolite	Formula (z = +1)	Predicted mass	Observed mass	Error (ppm)
1	$C_{17}H_{21}N_2O_5$	333.1445	333.1	n.d.
	$C_{17}H_{20}N_2O_5Na$	355.1270	355.1263	2.0
7	$C_{15}H_{19}N_2O_2$	259.1447	259.1447	0.0
	$C_{15}H_{18}N_2O_2Na$	281.1260	281.1	n.d.
8	$C_{15}H_{21}N_2O_2$	261.1603	261.1594	3.4
	$C_{15}H_{20}N_2O_2Na$	283.1417	283.1	n.d.

Table S2. High-resolution mass spectrometry. High-resolution mass data was acquired for either the M+H ion or the M+Na ion (n.d. = not determined).

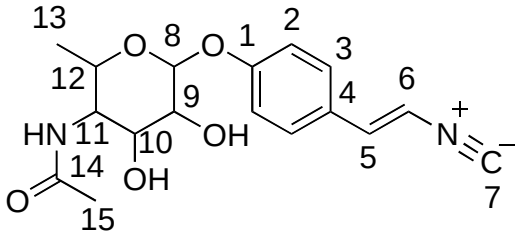

Structural Unit	Atom	δ_C (mult.)	δ_H (J in Hz)	gCOSY	gHMBC
Tyrosyl-derived unit	1	160.5			
	2	117.6 (CH)	7.06 d (8.7)	3	1, 2, 4
	3	129.3 (CH)	7.41 d (8.7)	2	1, 2, 3, 5
	4	128.1			
	5	137.5 (CH)	7.01 d (14.4)	6	3, 4, 6
	6	110.3 (CH)	6.50 d (14.4)	5	4, 5, 7
Isonitrile	7	164.7			
Sugar	8	102.0 (CH)	4.92 d (7.6)	9	1, 9
	9	72.0 (CH)	3.69 dd (7.7, 9.9)	8, 10	8, 10
	10	73.3 (CH)	3.78 dd (4.7, 10.0)	9, 11	9
	11	54.6 (CH)	4.30 dd (4.6, 1.0)	10, 12	10, 12, 14
	12	71.0 (CH)	3.95 dq (1.2, 6.0)	11, 13	8, 10, 11, 13
	13	17.0 (CH_3)	1.13 d (6.4)	12	11, 12
N-acetyl	14	174.6			
	15	22.9 (CH_3)	2.05 s		14

Table S3. ^{1}H and ^{13}C data for **1** in CD_3OD referenced to solvent. $[\alpha]_D$ = -21.8, c = 0.11, MeOH

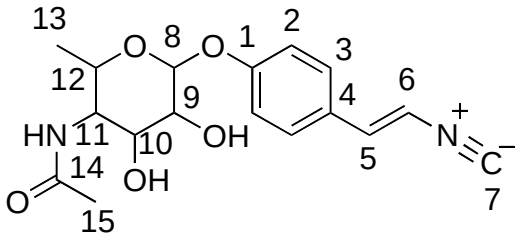

Structural Unit	Atom	δ_C (mult.)	δ_H (J in Hz)	gCOSY	gHMBC
Tyrosyl-derived unit	1	158.5			
	2	115.8 (CH)	7.01 d (8.8)	3	1, 2, 3, 4
	3	128.4 (CH)	7.48 d (8.8)	2	1, 2, 3, 5
	4	128.5			
	5	135.9 (CH)	7.12 d (14.3)	6	3, 4, 6
	6	109.6 (CH)	6.79 d (14.4)	5	4, 5, 7
Isonitrile	7	164.2			
Sugar	8	99.9 (CH)	4.91 d (7.4)	9	1, 9
	9	69.8 (CH)	3.59 m	8	8, 10
	OH		3.59 m		
	10	69.8 (CH)	3.59 m	11	9
	OH		4.10		
	11	52.3 (CH)	4.10 dd (9.3, 1.9)	10, NH	12, 14
	12	69.4 (CH)	3.90 dq (1.5, 6.3)	12	8, 10, 11, 13
	13	16.4 (CH_3)	1.00 d (6.4)	12	11, 12
N-acetyl	NH		7.58 d (9.7)	11	11, 14
	14	170.7			
	15	22.3 (CH_3)	1.90 s		14

Table S4. ^{1}H and ^{13}C data for **1** in $(CD_3)_2SO$ referenced to solvent.

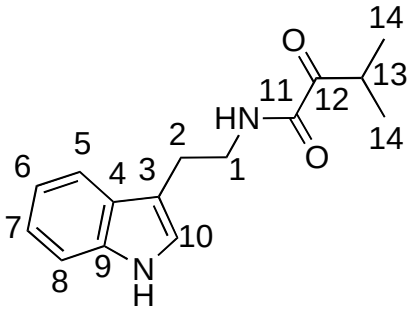

Structural Unit	Atom	δ_C (mult.)	δ_H (J in Hz)	gCOSY	gHMBC
Indole	NH		7.05 br d (2.2)	1, 2 w	
	1	39.5 (CH_2)	3.64 q (6.8)	NH, 2	2, 3, 11
	2	25.4 (CH_2)	3.03 t (6.9)	1, NH w	1, 3, 4, 10
	3				
	4				
	5	118.7 (CH)	7.61 dd (7.9, 0.6)	6	3, 4 w, 7, 9
	6	119.7 (CH)	7.14 td (7.6, 0.9)	5, 7	4, 8
	7	122.5 (CH)	7.22 td (7.7, 1.0)	6, 8	5, 9
	8	111.4 (CH)	7.38 d (8.1)	7	4, 6
	9				
	NH		8.03 br s	10	
	10	122.0 (CH)	7.05 br d (2.2)	NH	3, 4, 9
Side chain	11				
	12				
	13	34.1 (CH)	3.60 m	14	12, 14
	14	17.7 (CH_3)	1.12 d (6.9)	13	12, 13, 14

Table S5. ^{1}H and ^{13}C data for **7** in $CDCl_3$ referenced to solvent.

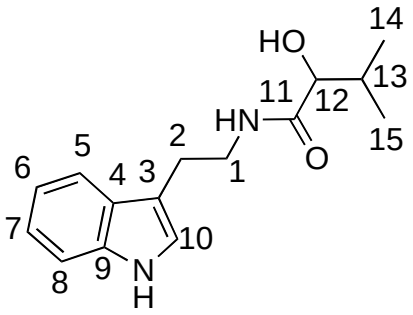

Structural Unit	Atom	δ_C (mult.)	δ_H (J in Hz)	gCOSY	gHMBC
Indole	NH		7.76 t (5.9)	1, 2 w	1, 11
	1	38.5 (CH_2)	3.40 m	NH, 2	2, 3, 11
	2	25.1 (CH_2)	2.83 td (7.5, 2.3)	1, NH w	1, 3, 4, 10
	3				
	4				
	5	118.1 (CH)	7.56 d (7.8)	6	3 w, 7, 9
	6	117.9 (CH)	6.97 td (7.5, 0.9)	5	4, 8
	7	120.6 (CH)	7.06 td (7.5, 1.0)	8	5, 9
	8	111.0 (CH)	7.33 d (8.1)	7	4, 6
	9				
	NH		10.79 s	10	8
	10	122.1 (CH)	7.14 d (2.2)	NH	3, 4, 9
Side chain	11				
	12	74.9 (CH)	3.66 t (3.8)	13, OH	
	OH		5.32 d (5.1)	12	
	13	30.8 (CH)	1.98 m	12, 14/15	
	14/15	18.8 (CH_3) 15.91 (CH_3)	0.89 d (6.9) 0.74 d (6.8)	13 13	12, 13, 15 12, 13, 14

Table S6. ^{1}H and ^{13}C data for **8** in $(CD_3)_2SO$ referenced to solvent.

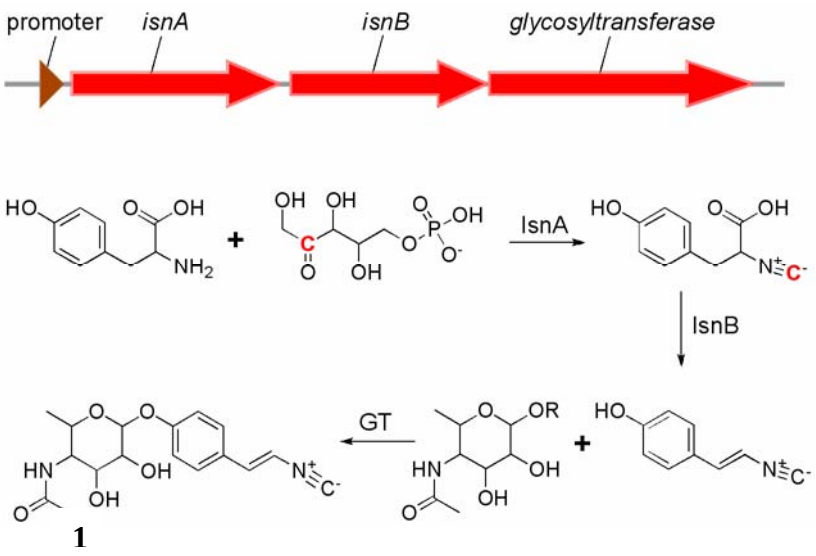

Figure S3. Proposed biosynthesis of rhabduscin (1) in *X. nematophila* and *P. luminescens.* The biosynthetic gene cluster in *X. nematophila* was identified by its characteristic isonitrile-forming biosynthetic genes, *isnA* and *isnB* [23-25]. The candidate isocyanide synthesizing proteins IsnA and IsnB and a glycosyltransferase homolog are encoded in the small *X. nematophila* biosynthetic operon shown above (*X. nematophila*: Xn_1221, Xn_1222, and Xn_1223; homologs were also detected in *P. luminescens*: Plu2816, Plu2817, and Plu1762). R = GT leaving group. Installation of the isocyanide group onto tyrosine by IsnA provides the substrate for IsnB, which catalyzes an oxidative decarboxylation. The glycosyltransferase completes the pathway by attaching the amino sugar.

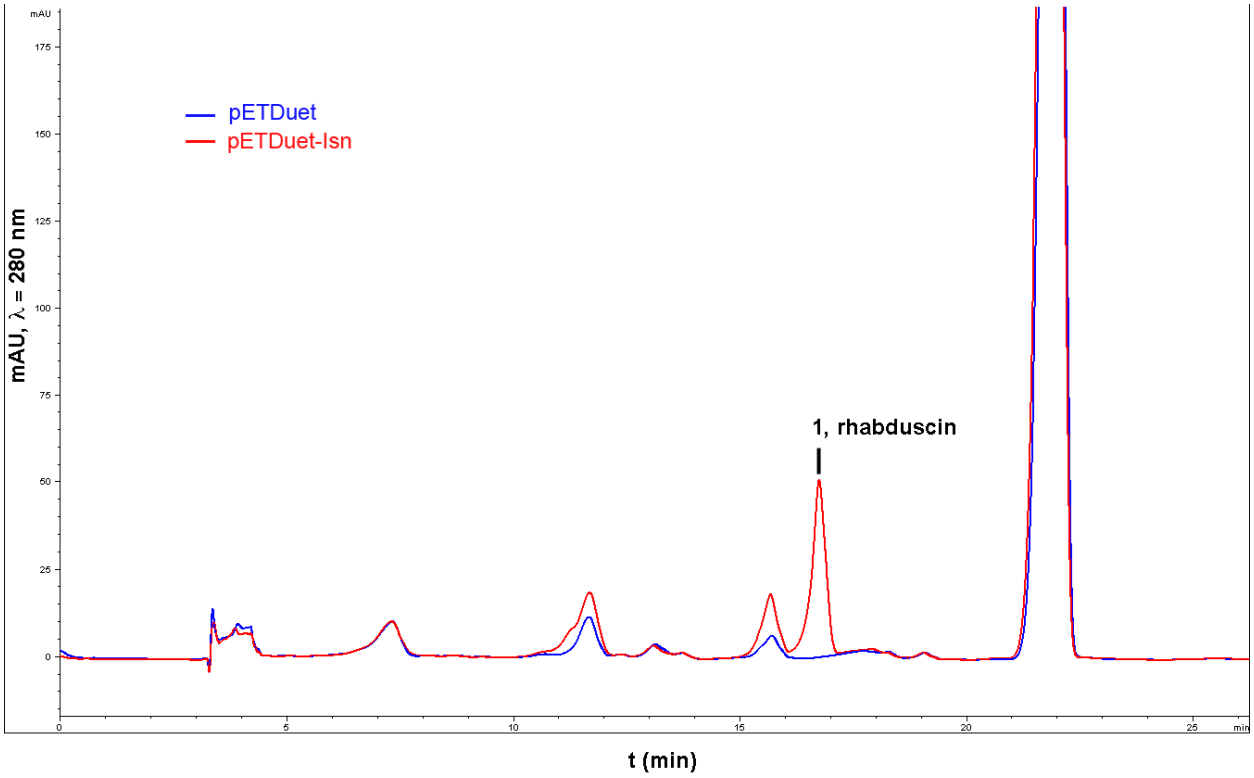

Figure S4. Heterologous expression of *X. nematophila* rhabduscin (1) biosynthetic gene cluster. The candidate rhabduscin biosynthetic gene cluster illustrated in Fig. S3 was cloned and heterologously expressed in *E. coli*. Rhabduscin produced in *E. coli* was detected by HPLC and confirmed by retention time, UV-visible, and MS comparison to the natural product. *E. coli* harboring the biosynthetic gene cluster exhibited rhabduscin (**1**) production by HPLC (red, pETDuet-Isn), but it was not detected in *E. coli* harboring the control plasmid (blue, pETDuet).

Heterologous expression of rhabduscin. The *X. nematophila* isonitrile cluster was amplified using primer pairs X.nem-Isn5 and X.nem-Isn3 (Table S7). The resulting PCR product was digested with NcoI and BamHI and inserted into the corresponding sites in pETDuet-1 (Novagen) to generate pETDuet-Isn. pETDuet-Isn and pETDuet-1 were individually transformed into BL21 Star^{TM} (DE3) pLysS (Invitrogen). Transformants were selected on LB agar containing 25 μg/mL chloramphenicol.

E. coli transformants were grown in suspension (5 mL of LB, 25 μg/mL chloramphenicol) at 37 °C and 250 rpm to an OD_{600} = 0.6-0.8. Expression of the cluster was induced by the addition of IPTG (1 mM final) and the cultures were incubated at 20 °C and 250 rpm for an additional 36 hours. Rhabduscin (**1**) was extracted with ethyl acetate and analyzed exactly as described in the Metabolite Stimulation section above. The HPLC retention time, UV-visible chromophore, and mass were identical to the natural product **1** produced in either *X. nematophila* or *P. luminescens*.

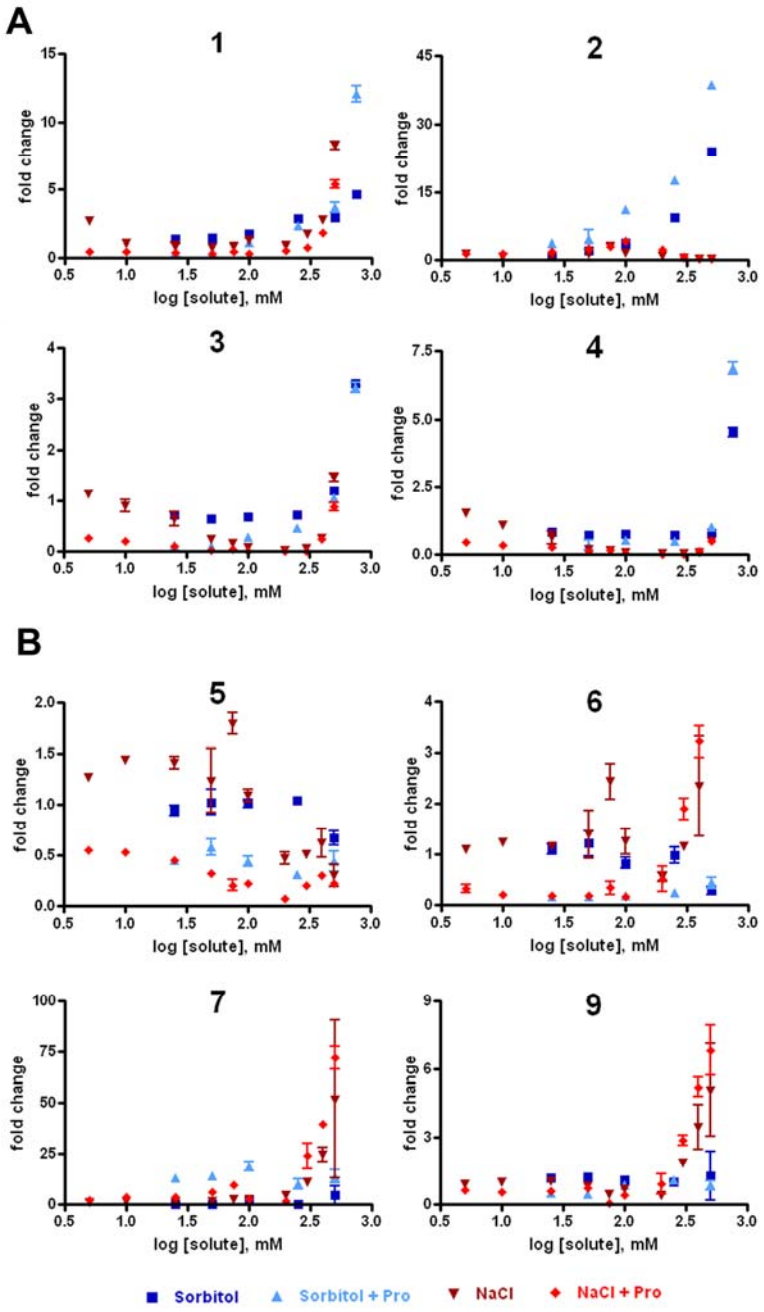

Figure S5. Osmoregulated secondary metabolic flux. Osmotic stressors (sorbitol or NaCl) were added to the medium to evaluate osmoregulated metabolites in *P. luminescens* (**A**) and *X. nematophila* (**B**). The fold change of individual metabolites (numbers correspond to metabolites in Fig. 1) is compared to control cultures lacking osmotic stressors (error bars = s.d.). Sorbitol titration experiments (0-750 mM sorbitol) were performed in a rich tryptone-yeast extract based medium with a reduced salt concentration (2 g/L tryptone, 5 g/L yeast-extract, and 10 mM NaCl) with 50 mM L-proline (light blue) or without 50 mM L-proline (dark blue). *X. nematophila* was incapable of growing in the 750 mM sorbitol liquid medium, but was analyzed from 0-500 mM. NaCl titration experiments (0-500 mM NaCl) were performed in a rich tryptone-yeast extract based medium (2 g tryptone, 5 g yeast-extract per L) with 50 mM L-proline (red) or without 50 mM L-proline (reddish brown). Osmotic challenges mimicking the physiology of the insect host contributed to the metabolite regulation, and the accumulation of L-proline provided an enhanced effect. However, proline alone in non-osmotically challenged cultures shows more drastic fold changes in metabolite production than osmotically challenged cultures lacking proline (Figs. 3-4), arguing that osmolarity alone is not sufficient for the regulation of metabolites once in the insect host environment.

Osmoregulated secondary metabolic flux. Osmolarity is an underlying physiological parameter thought to control virulence in several bacterial pathogens [26]. Certain amino acids (*e.g.* L-proline), sugars, polyols and derivatives thereof are often acquired or synthesized to high intracellular concentrations (up to molar amounts) to manage water losses due to environmental osmotic stresses [27]. These compatible solutes have minimal effect on macromolecular structure and allow bacteria to manage their turgor pressure in hyperosmotic environments. Because the hemolymph has long been known to contain high solute and inorganic salt concentrations [22], we challenged *P. luminescens* and *X. nematophila* cultures to osmotic stressors with and without proline. When osmolarity (but not salinity) was altered by the addition of the solute sorbitol, *P. luminescens* drastically increased metabolite production (including rhabduscin) when the polyol was present at higher concentrations, and L-proline provided an enhanced effect (Fig. S5). Conversely, *X. nematophila* cultures exhibited reduced metabolite production and poor growth characteristics when challenged by sorbitol. By altering the salinity using NaCl, the reverse effect was observed in the two bacteria. Increased osmotic stress by salt generally stimulated metabolite production in *X. nematophila* cultures, and L-proline provided further stimulation, whereas metabolic profiles were not significantly altered by NaCl in *P. luminescens* cultures. Nematophin (**5**) production again decreased with salt as in proline- or hemolymph-induced cultures. This reciprocal production profile suggests that osmolarity does contribute to the metabolic shift. L-proline is likely a preferred compatible solute based on its availability in the hemolymph, but high osmotic stress was still capable of partially inducing metabolite production in the absence of L-proline. Supporting this notion, hypoosmotic conditions were previously described to maintain a stable secondary form that does not produce antibiotics in rich medium [6]. This data indicates that osmotic challenges mimicking the physiology of the insect host contribute to the metabolite regulation, and the accumulation of L-proline provides an enhanced effect. The drastically different behaviors that the two genera exhibit, however, exemplifies their dissimilar downstream regulatory networks.

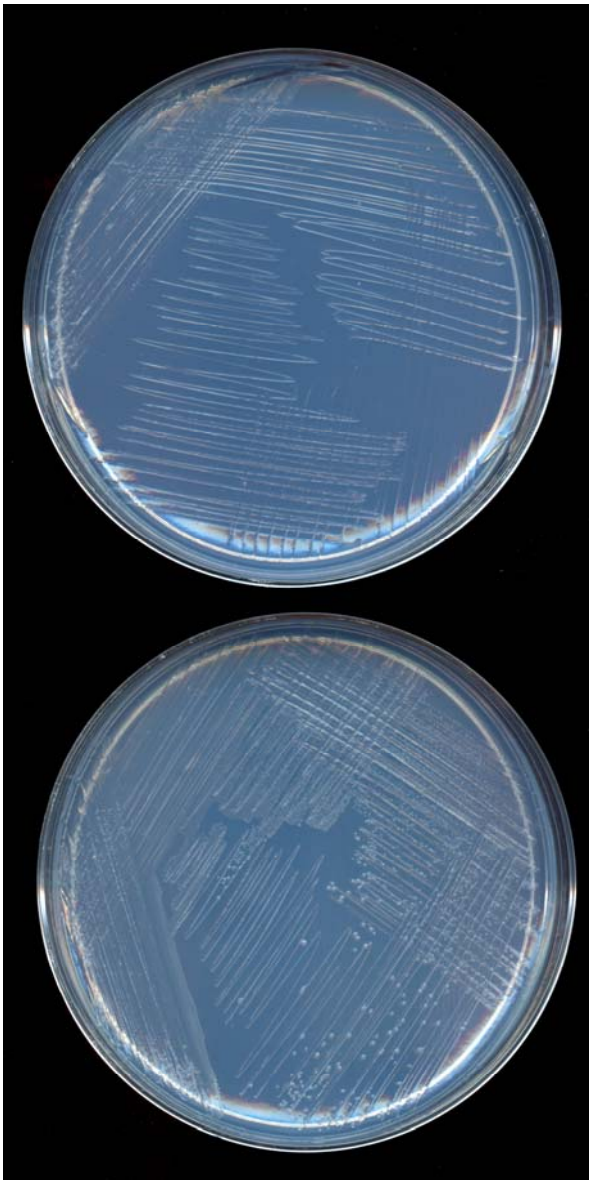

Figure S6. Proline auxotrophy complementation. Complementation of proline auxotroph *E. coli* WG389 with *P. luminescens putP* (pCPutP, bottom) fully restored growth, whereas introduction of the empty vector (pCR2.1, top) did not support growth.

The *putP* sequence and upstream intergenic region were amplified by PCR using primer pairs PutP5 and PutP3 (Table S7). The product was cloned into pCR2.1 TOPO (Invitrogen) to generate pCPutP. The gene was inserted downstream of the vector's lac promoter. pCPutP and control vector pCR2.1 (circularized) were individually transformed into the proline auxotroph strain, *E. coli* WG389 [28]. Transformants were selected on LB supplemented with 50 μg/mL kanamycin and 25 mM L-proline. Single colonies were then monitored over a 2-3 day period at 37 °C for genetic complementation ability on a modified MOPS minimal medium as illustrated above. These auxotrophic restoration experiments were performed as previously described [28].

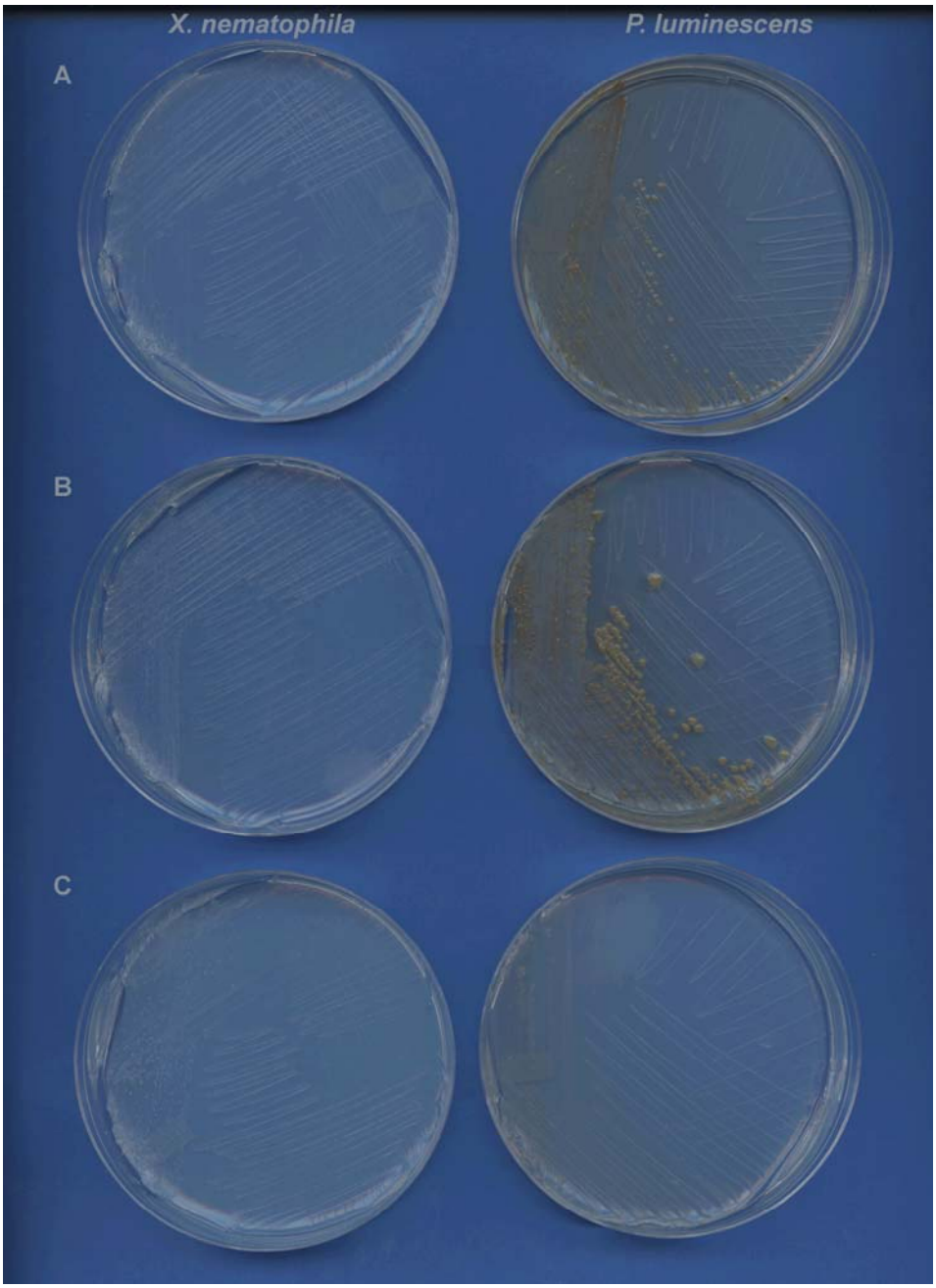

Figure S7. Proline utilization as a sole carbon source. Individual *P. luminescens* and *X. nematophila* colonies were streaked onto MOPS minimal medium [29], but with L-proline supplemented as the sole carbon source. *P. luminescens* (right) and *X. nematophila* (left) were grown on a MOPS minimal medium with 0.1% glucose (A), 0.1% L-proline (B), and 200 mM L-proline (C) at 30 °C for one-week. *X. nematophila* formed larger macrocolonies on proline as the sole carbon source compared to glucose. *P. luminescens* formed larger macrocolonies on 0.1% L-proline compared to 0.1% glucose. Neither *P. luminescens* nor *X. nematophila* grew on control plates lacking a carbon source, and they also grew more quickly (2-3 days) on LB (data not shown).

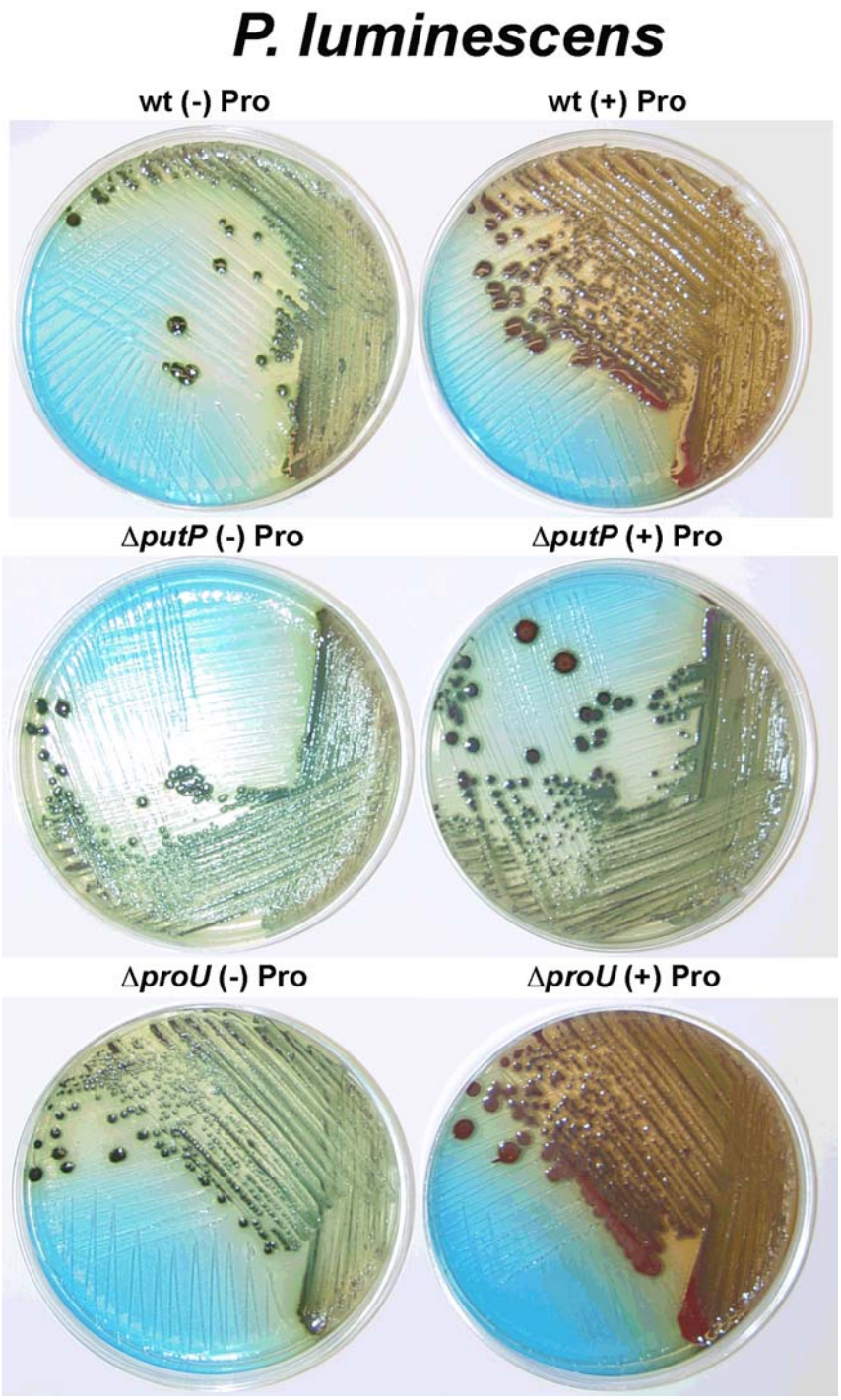

Figure S8. *P. luminescens* grown on low salt agar medium (2 g tryptone and 5 g yeast extract per L with and without 100 mM L-proline) in the presence of TTC and bromothymol blue (incubation time, 30 °C for 3-5 days). This growth condition was also illustrated in Fig. 5. Staining patterns reveal a reddening of wild type colonies and the Δ*proU* mutant upon proline supplementation, indicating increased reduction of TTC. A darkening of colonies is also observed with proline, indicating increased dye uptake. Given our differential metabolic observations, it is logical that the *P. luminescens* Δ*putP* culture with proline resembled the wild-type strain grown in the absence of proline.

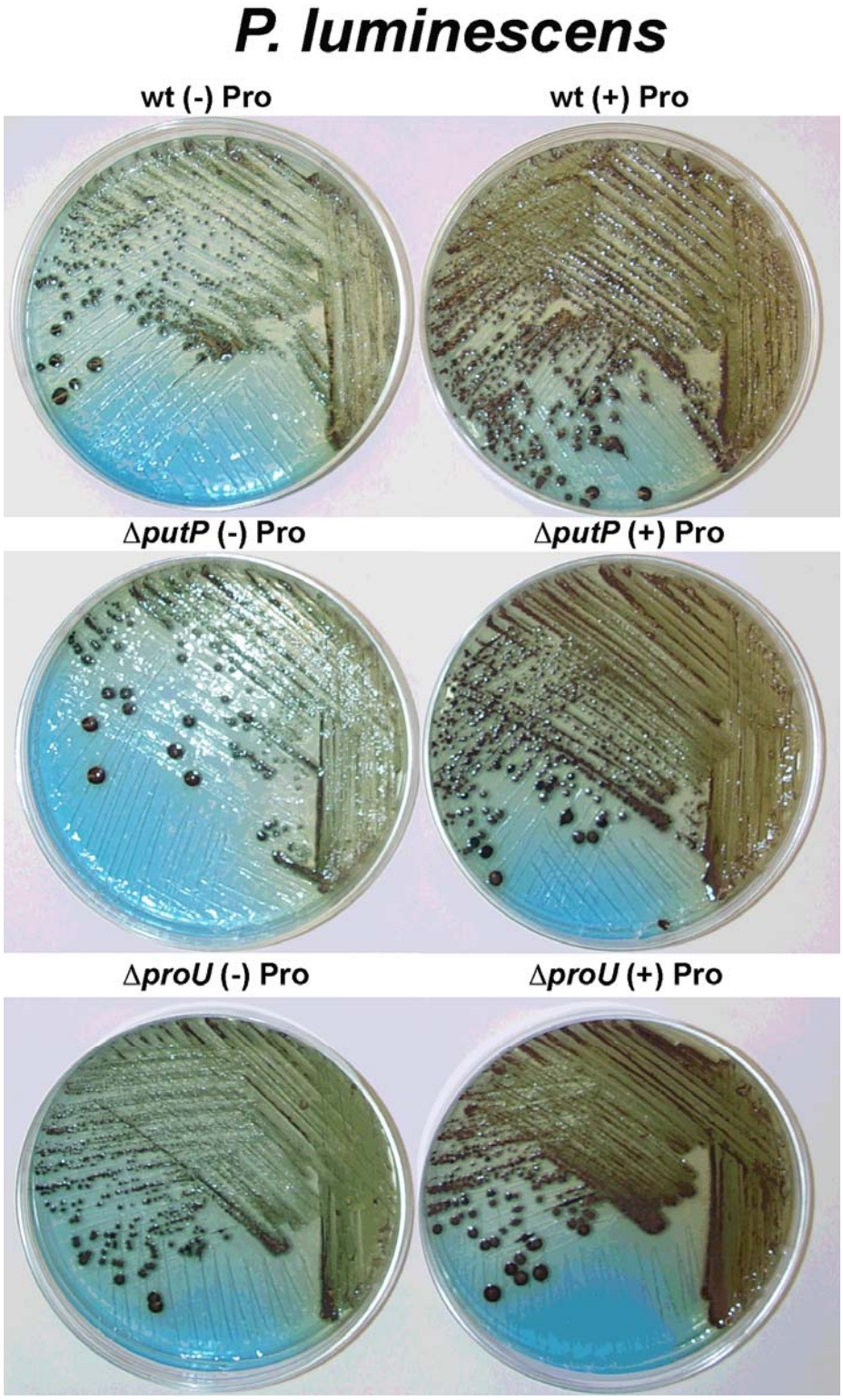

Figure S9. *P. luminescens* grown on medium salt agar medium (2 g tryptone, 5 g yeast extract, and 10 g NaCl per L with and without 100 mM L-proline) in the presence of TTC and bromothymol blue. Similar staining trends were observed when the bacteria were grown on varying salt concentrations.

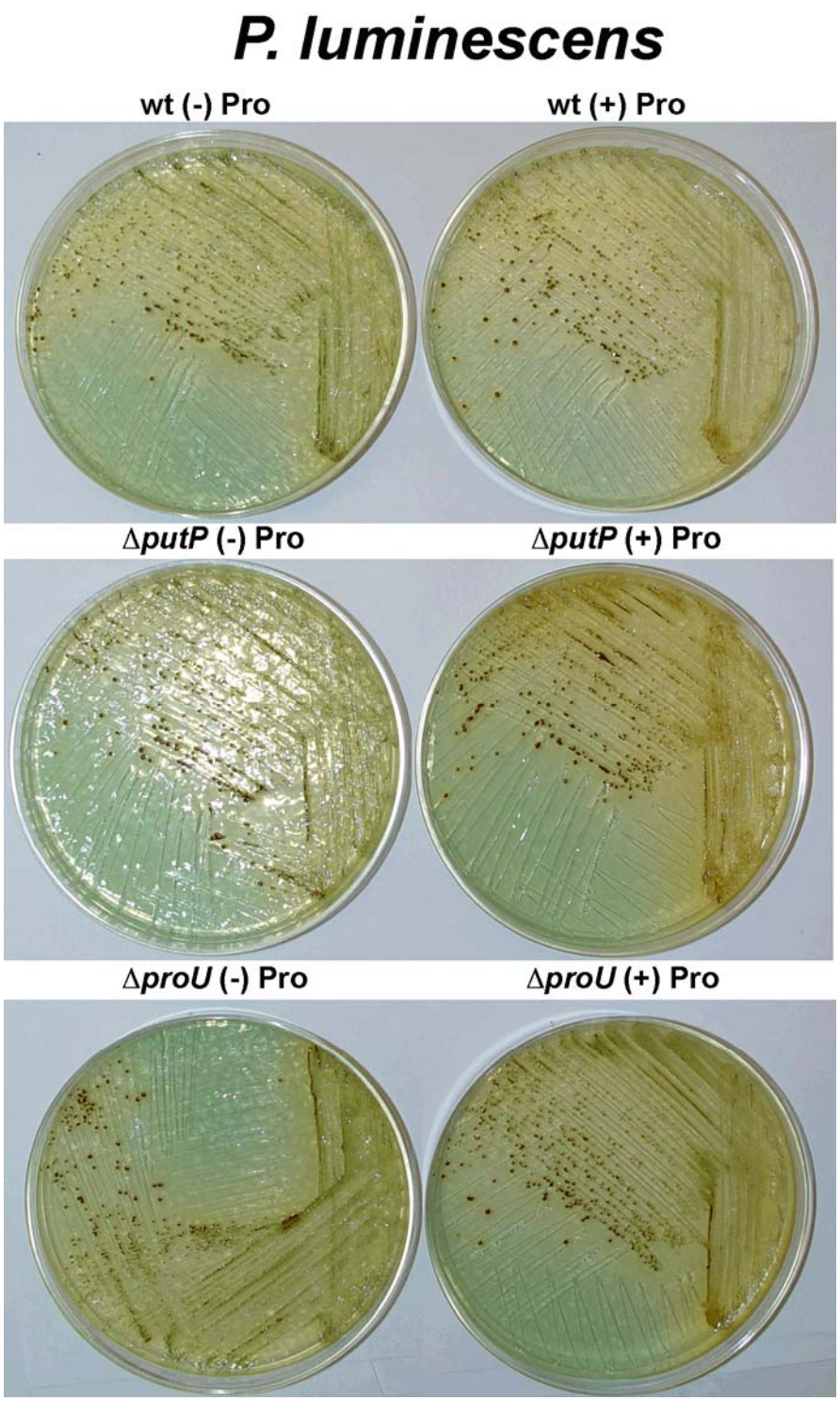

Figure S10. *P. luminescens* grown on high salt agar medium (2 g tryptone and 5 g yeast extract per L including 0.6 M NaCl with and without 100 mM L-proline) in the presence of TTC and bromothymol blue. The high osmotic stress reduced overall growth, but individual colonies growing on the proline supplemented plates were redder with a darker blue hue indicating increased dye uptake and reduction of TTC.

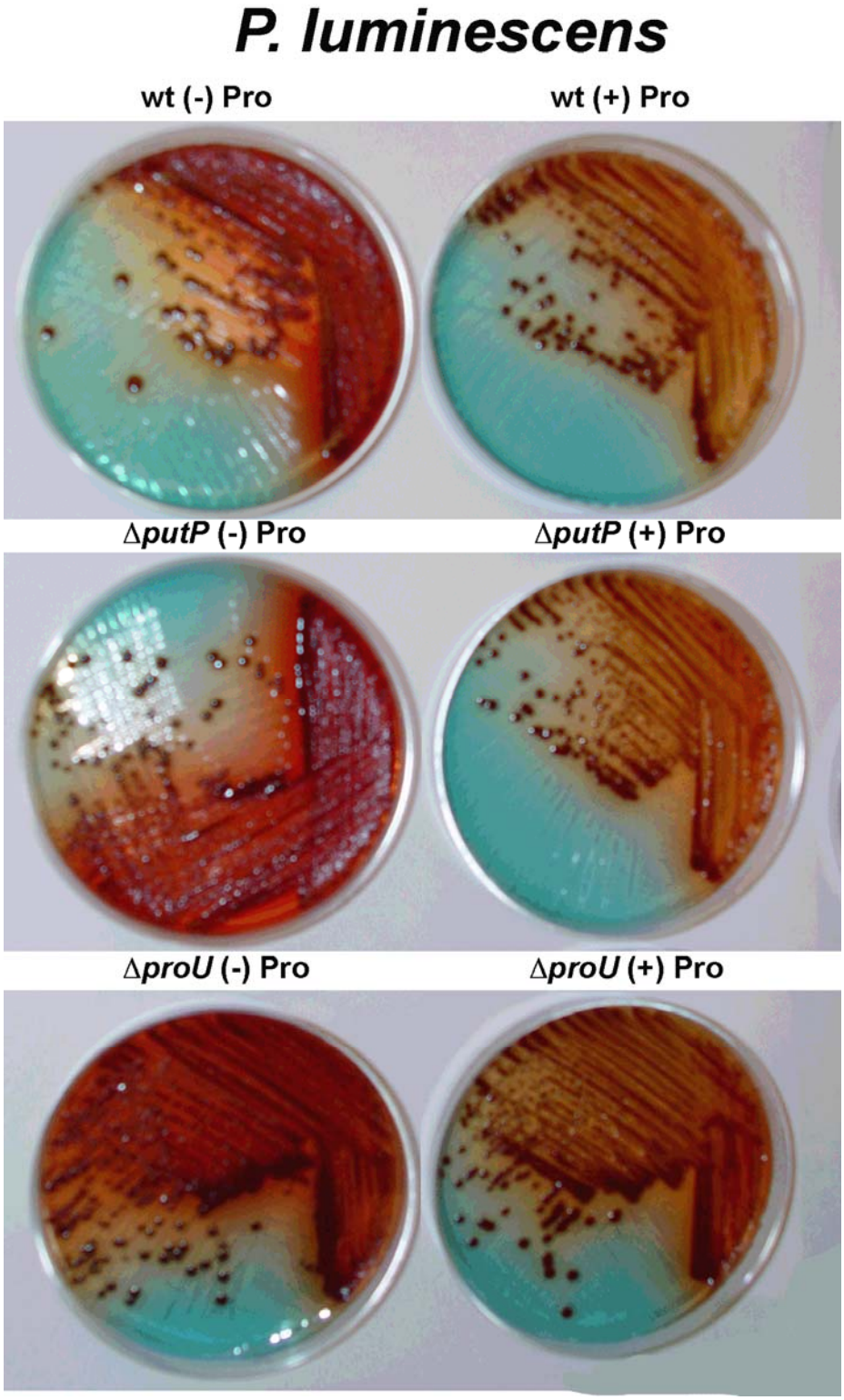

Figure S11. *P. luminescens* grown on high osmolarity agar medium (2 g tryptone and 5 g yeast extract per L including 0.75 M sorbitol with and without 100 mM L-proline) in the presence of TTC and bromothymol blue. The solute sorbitol increased reduction of TTC giving dark red colonies.

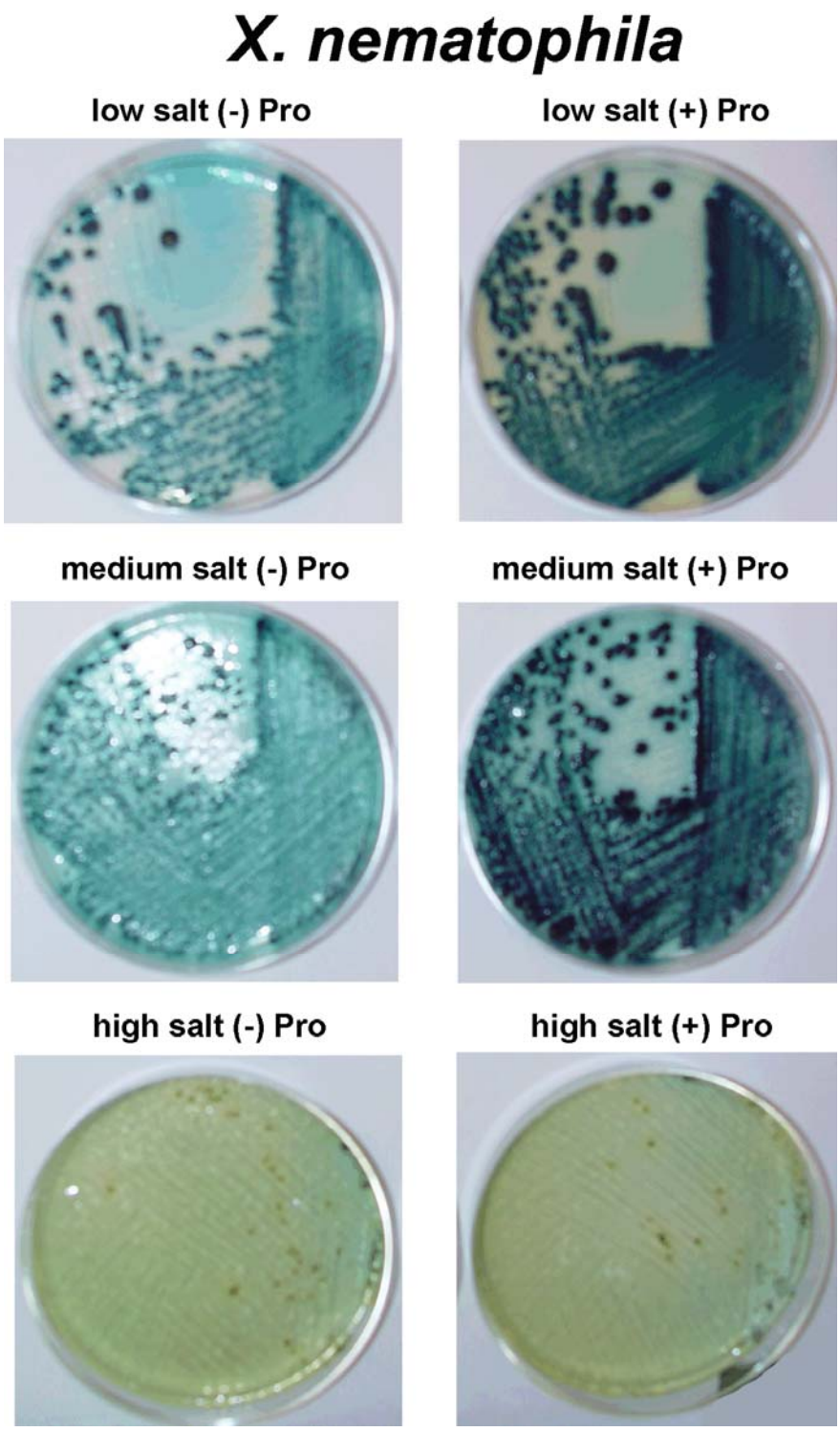

Figure S12. *X. nematophila* grown on low, medium, and high salt agar medium as described above with and without 100 mM L-proline in the presence of TTC and bromothymol blue. The addition of proline visually increased dye uptake and TTC reduction to give very dark colonies on low and medium salt plates. Individual colonies were slightly darker on the high salt plates with proline compared to the high salt plates lacking proline.

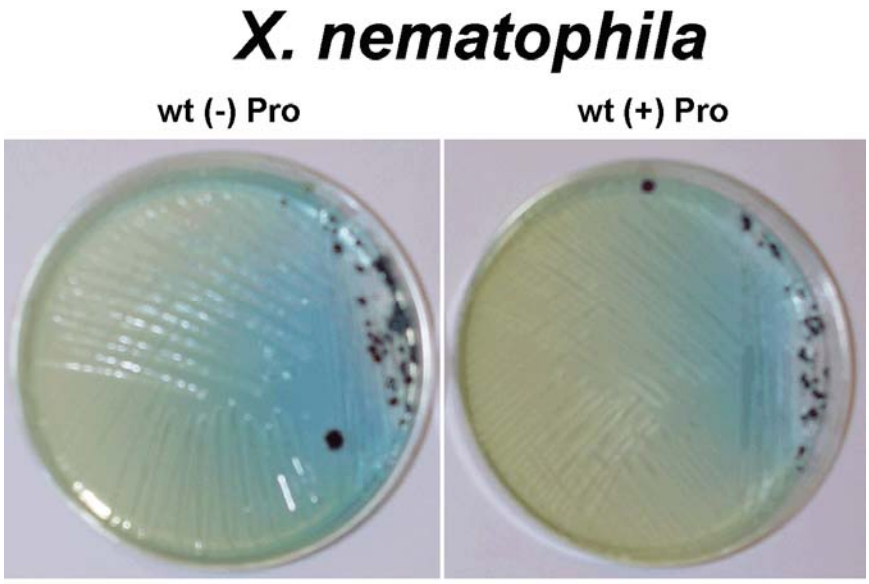

Figure S13. *X. nematophila* grown on high osmolarity sorbitol agar medium as described above with and without 100 mM L-proline in the presence of TTC and bromothymol blue. Under the conditions of the experiment, sorbitol caused poor growth characteristics for *X. nematophila*.

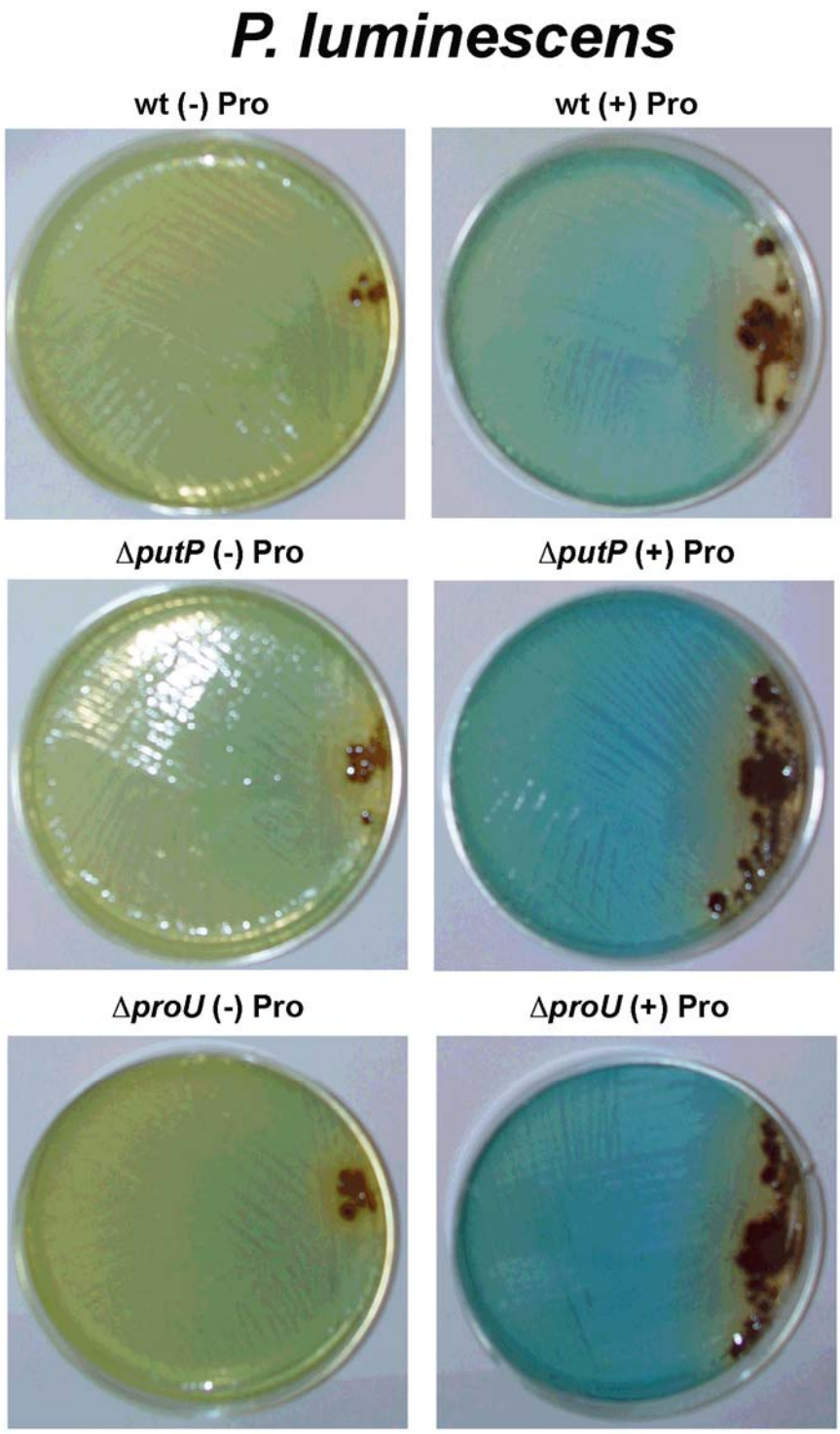

Figure S14. *P. luminescens* grown on low salt agar medium including 10 μM CCCP with and without 100 mM L-proline in the presence of TTC and bromothymol blue. Proline increased growth of *P. luminescens* on a low salt medium, presumably by providing an electron source to out-compete CCCP-dependent membrane energy diffusion.

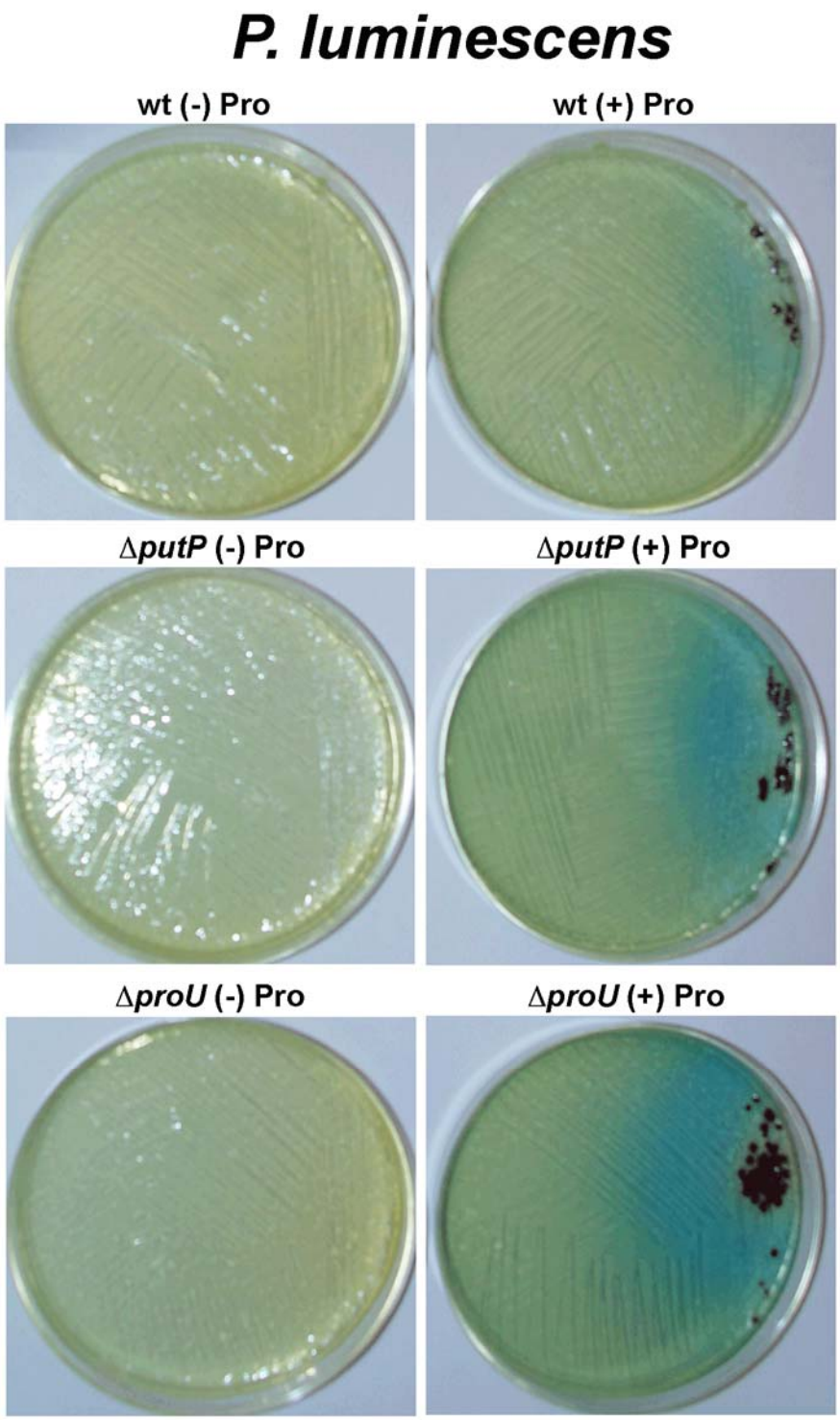

Figure S15. *P. luminescens* grown on medium salt agar medium including 10 μM CCCP with and without 100 mM L-proline in the presence of TTC and bromothymol blue. Proline partially rescued growth of *P. luminescens*, again by presumably providing an electron source to out-compete CCCP-dependent membrane energy diffusion.

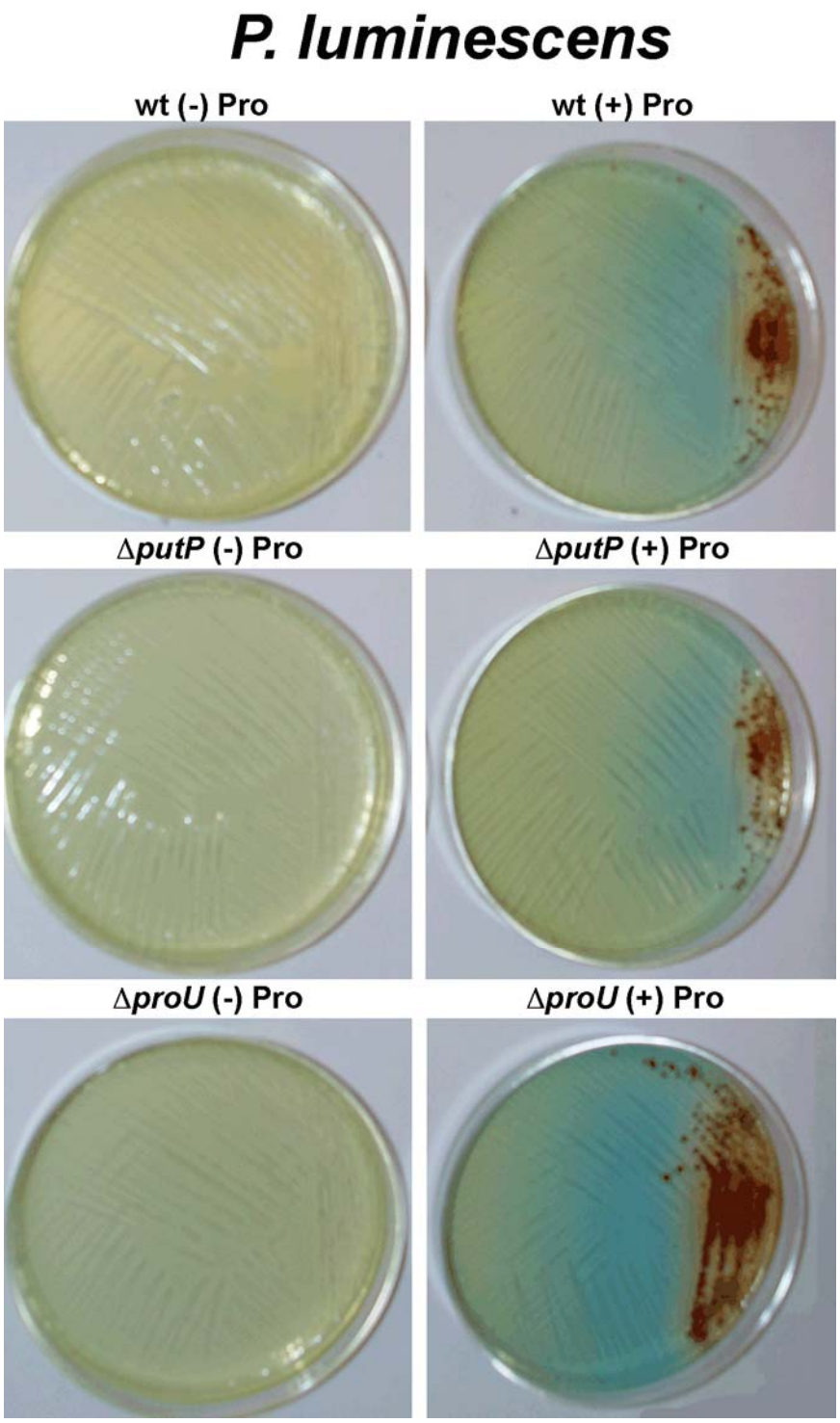

Figure S16. *P. luminescens* grown on high osmolarity sorbitol agar medium including 10 μM CCCP with and without 100 mM L-proline in the presence of TTC and bromothymol blue. Proline rescued growth of *P. luminescens* even under osmotic stress, presumably by providing an electron source to out-compete CCCP-dependent membrane energy diffusion and also likely acting as an osmolyte.

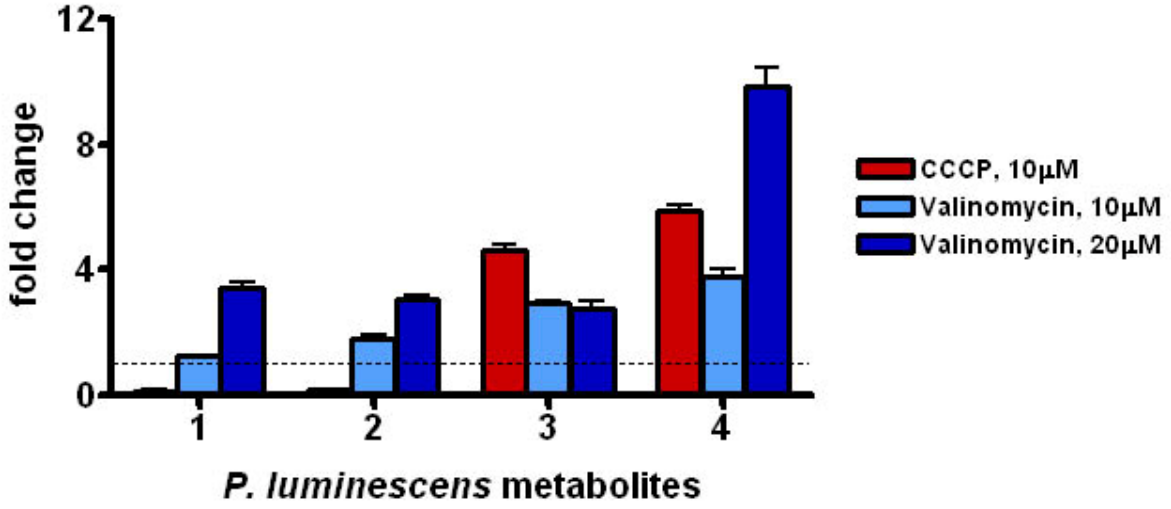

Figure S17. PMF and metabolite stimulation. To relate potential membrane energization to metabolite stimulation, we added PMF antagonists CCCP (diffuses both electrical and osmotic components of the PMF) and valinomycin (diffuses only the electrical component in the presence of potassium) to proline-supplemented mid-exponential suspension cultures of *P. luminescens*. Proline-supplemented (50 mM) suspension cultures of *P. luminescens* (2 g tryptone, 5 g yeast-extract, and 10 g NaCl per L base medium) were grown to mid-log phase (OD_{600} = 0.8, over 4-8 h) and then antagonized by 10 uM CCCP; 10 uM valinomycin and 150 mM KCl; or 20 uM valinomycin and 150 mM KCl. The perturbed cultures continued to grow for a total time of 72 hours (30 °C and 250 rpm) before the metabolites were extracted and quantified. The dashed line set at 1 represents the average metabolite production in control cultures stimulated by L-proline but lacking membrane diffusion agents. Numbers on the *x*-axis represent metabolites illustrated in Fig. 1. The membrane energy diffusion agents, administered at mid-log phase, caused substantial metabolite stimulation in *P. luminescens* stationary phase over proline-stimulated cultures alone (error bars = s.d. (+/-)).

Primer	Sequence (5′-3′)
PutP-A5	GTAAGAGCTC-AAGCTTCCGCAAGACACATTAGTGC
PutP-A3	CCTTTATTCCAATTTACC-GCAAGTTCTCCATAGTGTTATCTGTGTTTTG
PutP-B5	ACACTATGGAGAACTTGC-GGTAAATTGGAATAAAGGTAACCAACAAACCTC
PutP-B3	GTAAGAGCTC-GATAACCAAATTGCCCAATTTATTGATCC
ProU-A5	GTAA-GCATGC-AACTGAGATTGGTTACTTGTTTGTAACGGG
ProU-A3	AAGGAAAGTAACTATTTC-TACTTAGAACATTACAGTGAATTGGTATAAAACAATTC
ProU-B5	TTCACTGTAATGTTCTAAGTA-GAAATAGTTACTTTCCTTTCAATGGTTATTTAATGG
ProU-B3	GTAA-GCATGC-CTTATTATCCGAGATGAAGCCATTCACGG
PutP5-genome	ATTTTGTCGCGGATCAGCGCGTC
PutP3-genome	CCGGATTACTGAATATTCGTAAACGCG
ProU5-genome	GTAGTGATAAGGTTTACAATAGAGCCAAGTAATTG
ProU3-genome	TACCTATGTATTGGTCAAGTCGAGGAATATTAAC
PutP5	TAACAGCATGGGAATGGCTTGTGTTTC
PutP3	TTATTTAGTCTTGTATTGCGCCTCAGCATC
X.nem-Isn5	GTTAAAAAT-CC-ATGGAATATTTTGATATAGAAGAAGTGTCGAGCA
X.nem-Isn3	GTTAAAAAT-GGATCC-TTATGCCGATTGAGCAATCAGCTCATTAA

Table S7. Oligonucleotide sequences used in cloning experiments.

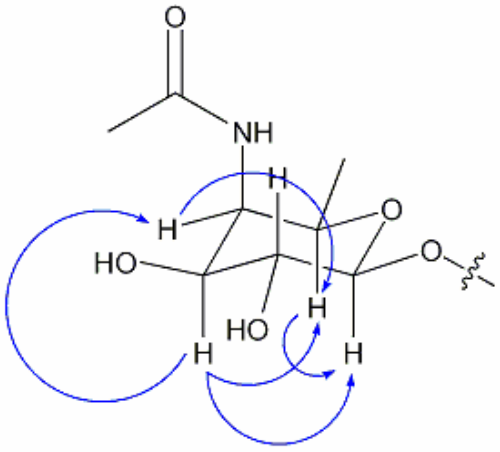

Figure S18. Key ROESY correlations of 1.

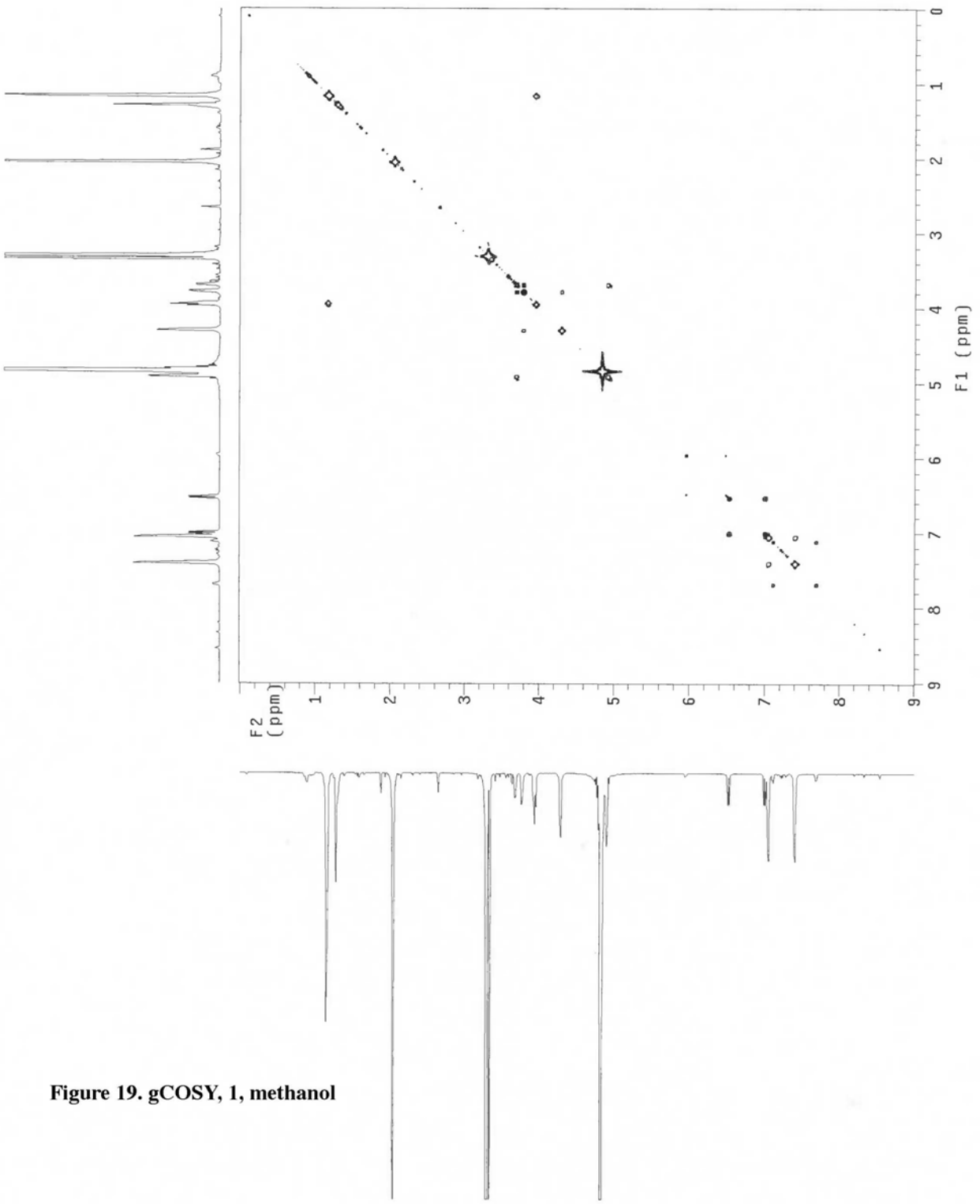

Figure 19. gCOSY, 1, methanol

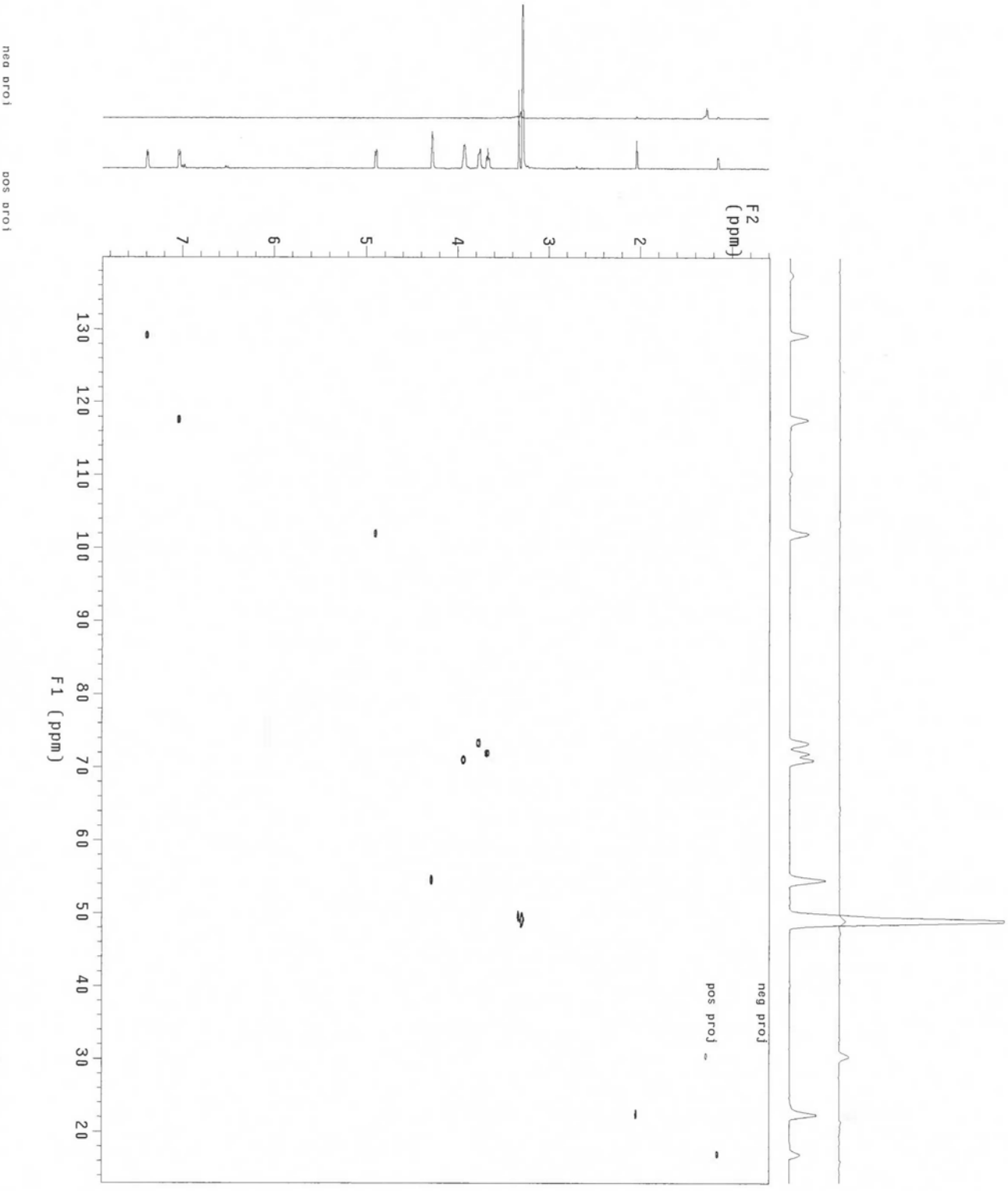

Figure 20. HSQC, 1, methanol

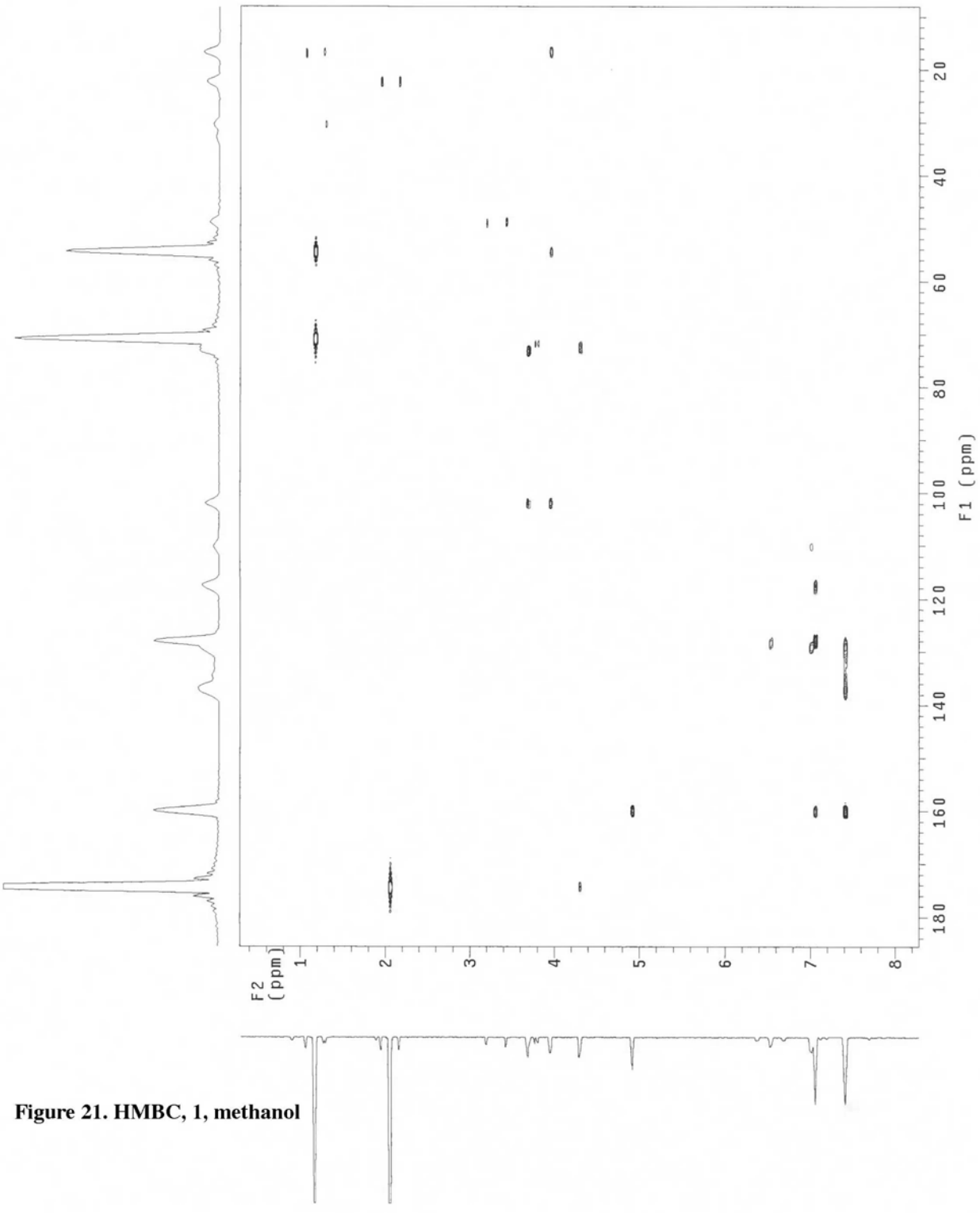

Figure 21. HMBC, 1, methanol

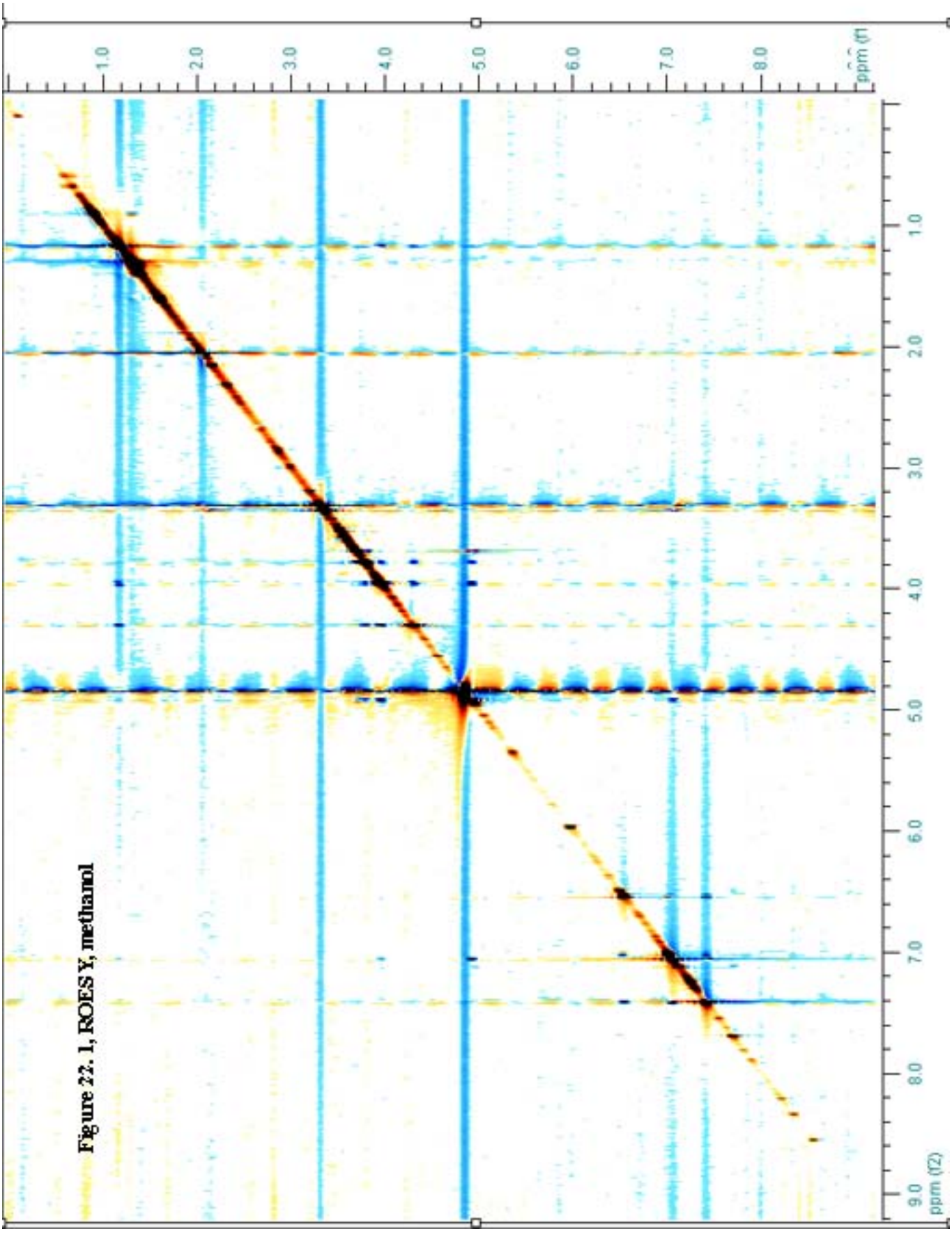

Figure 22. 1, ROESY, methanol

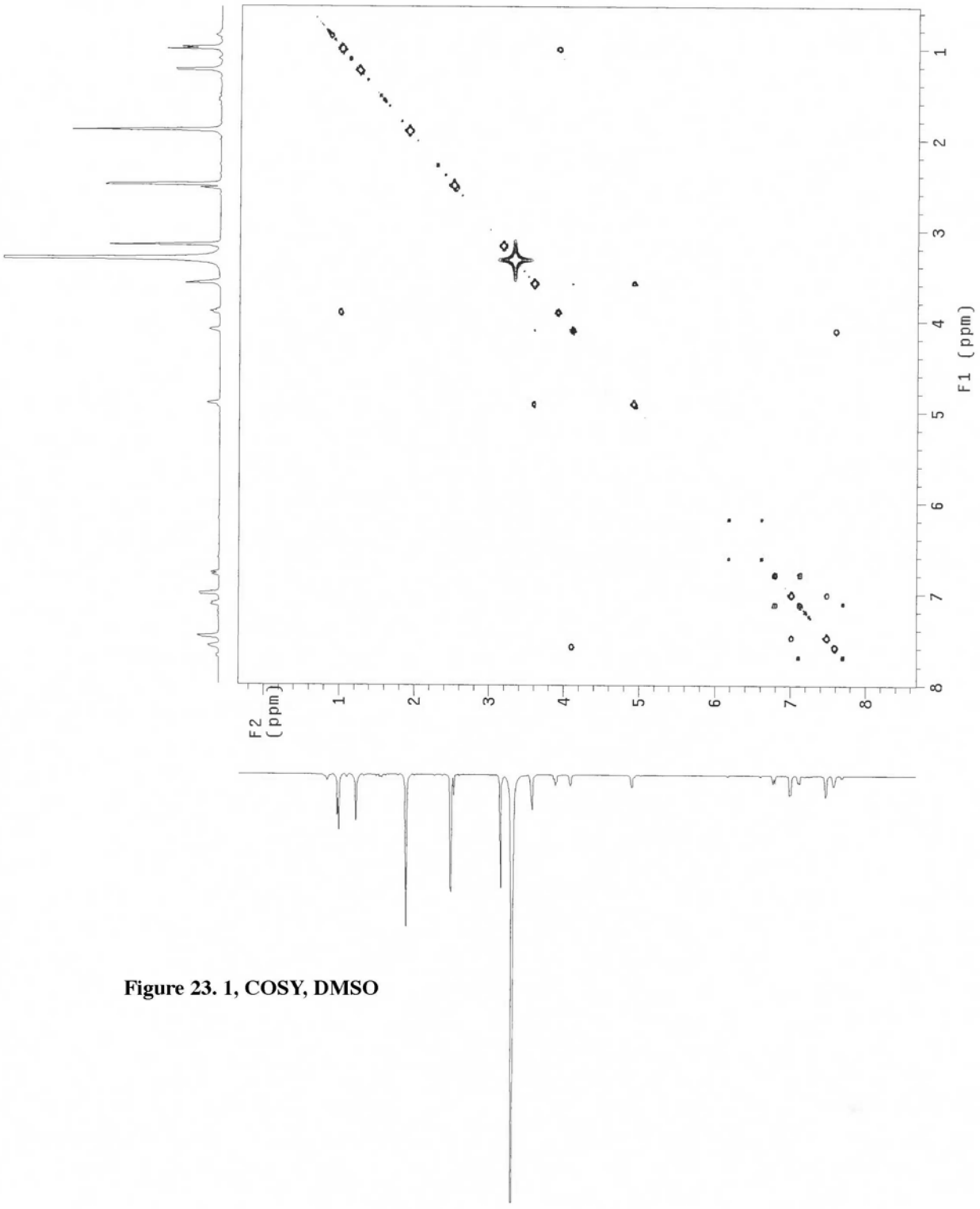

Figure 23. 1, COSY, DMSO

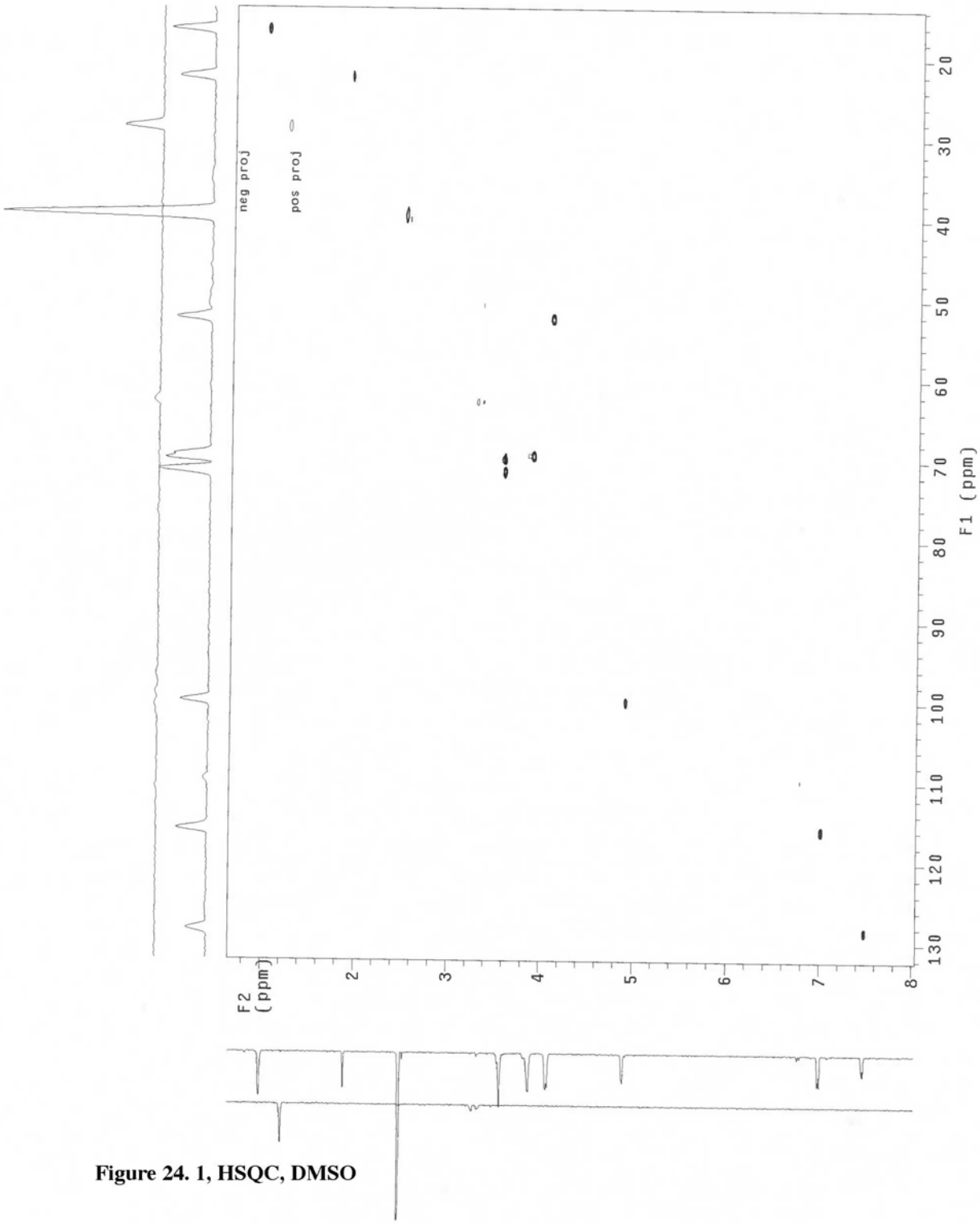

Figure 24. 1, HSQC, DMSO

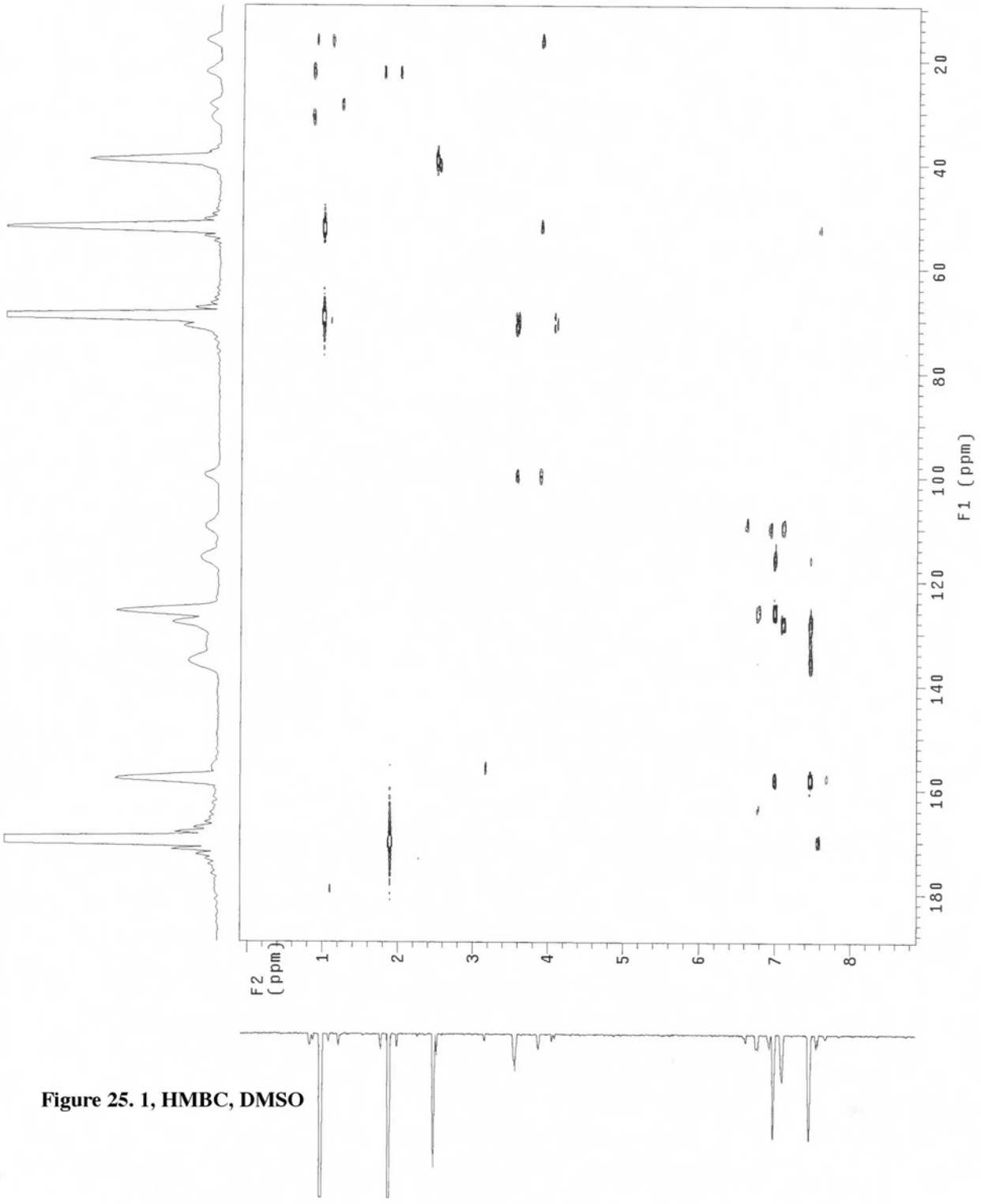

Figure 25. 1, HMBC, DMSO

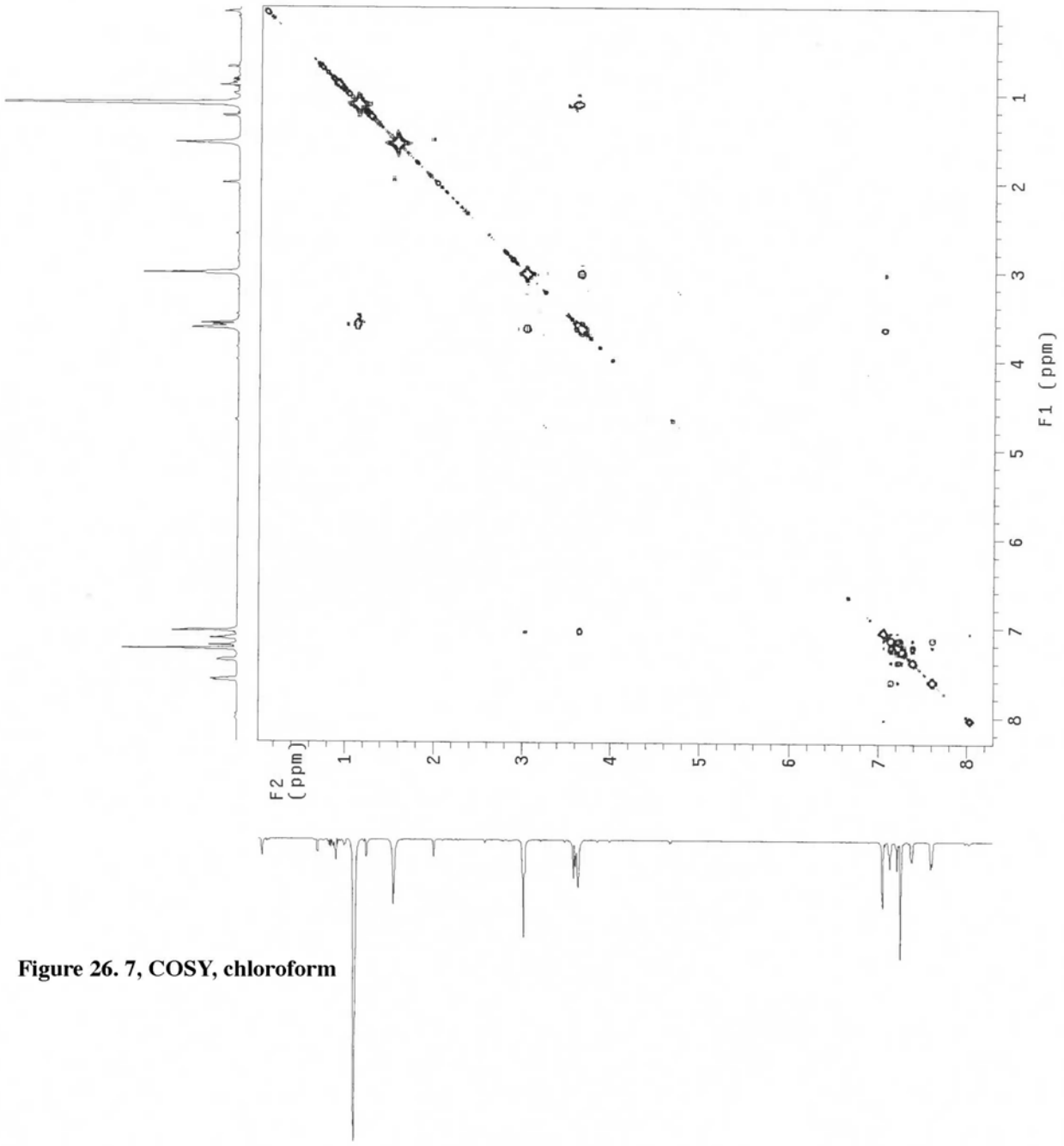

Figure 26. 7, COSY, chloroform

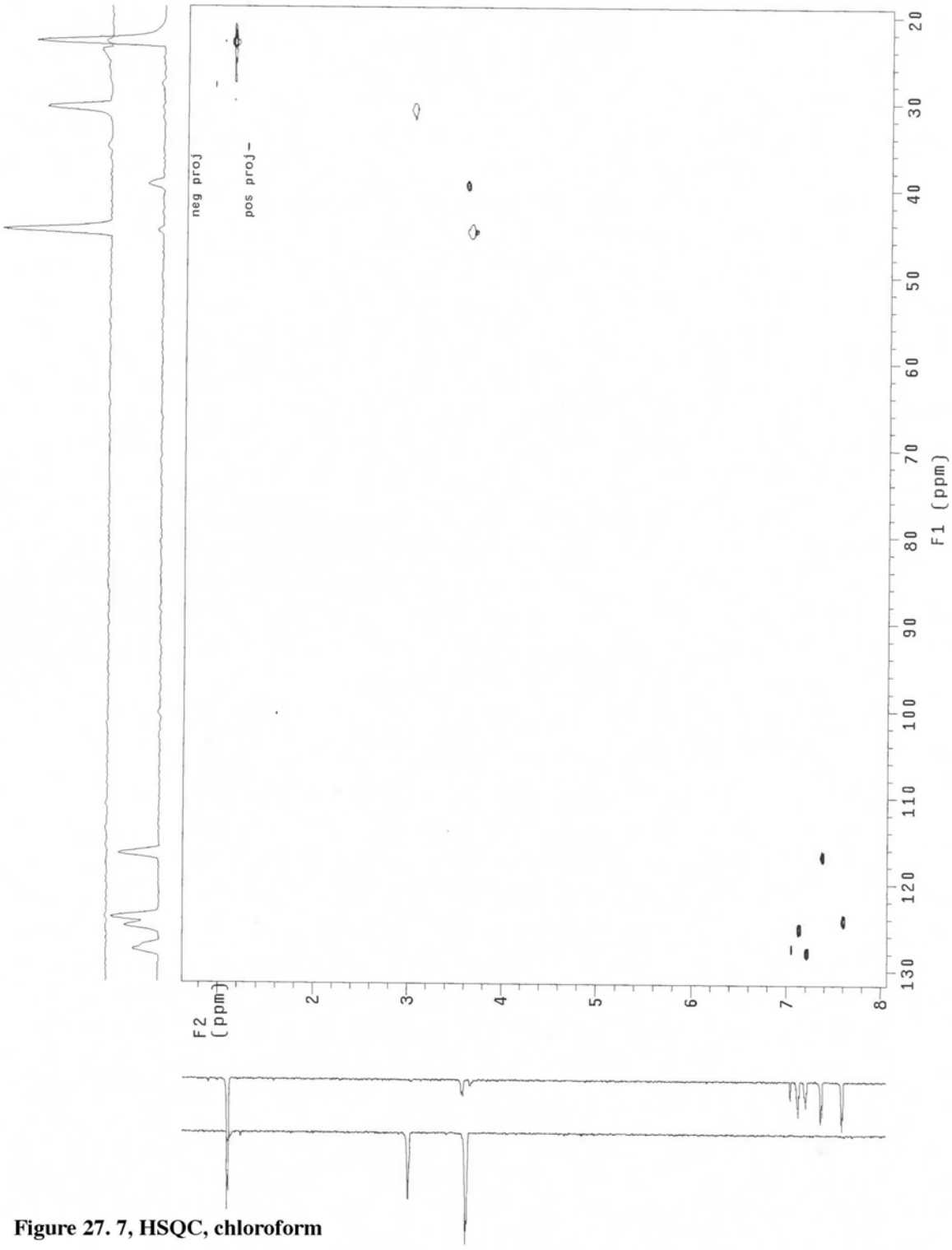

Figure 27. 7, HSQC, chloroform

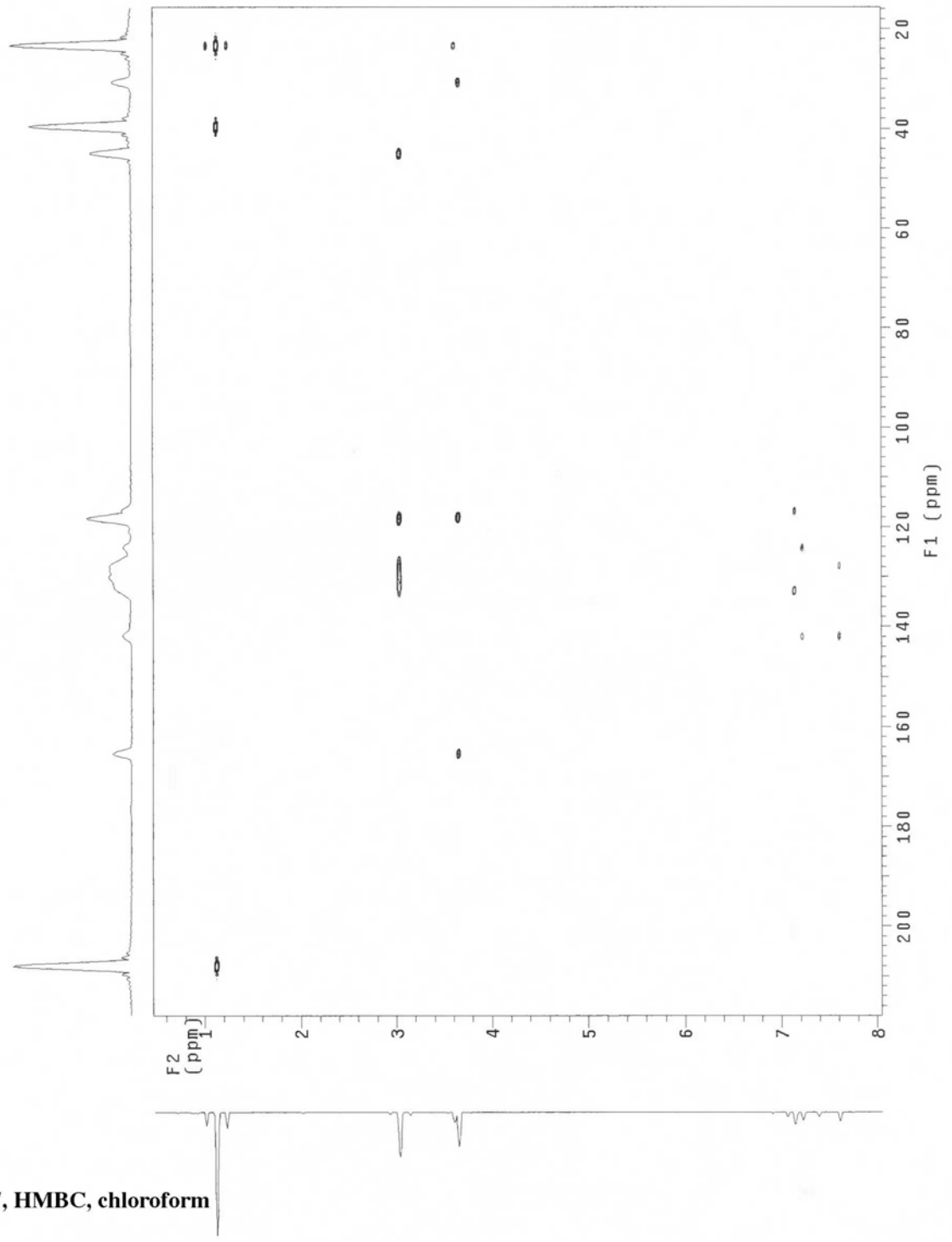

Figure 28. 7, HMBC, chloroform

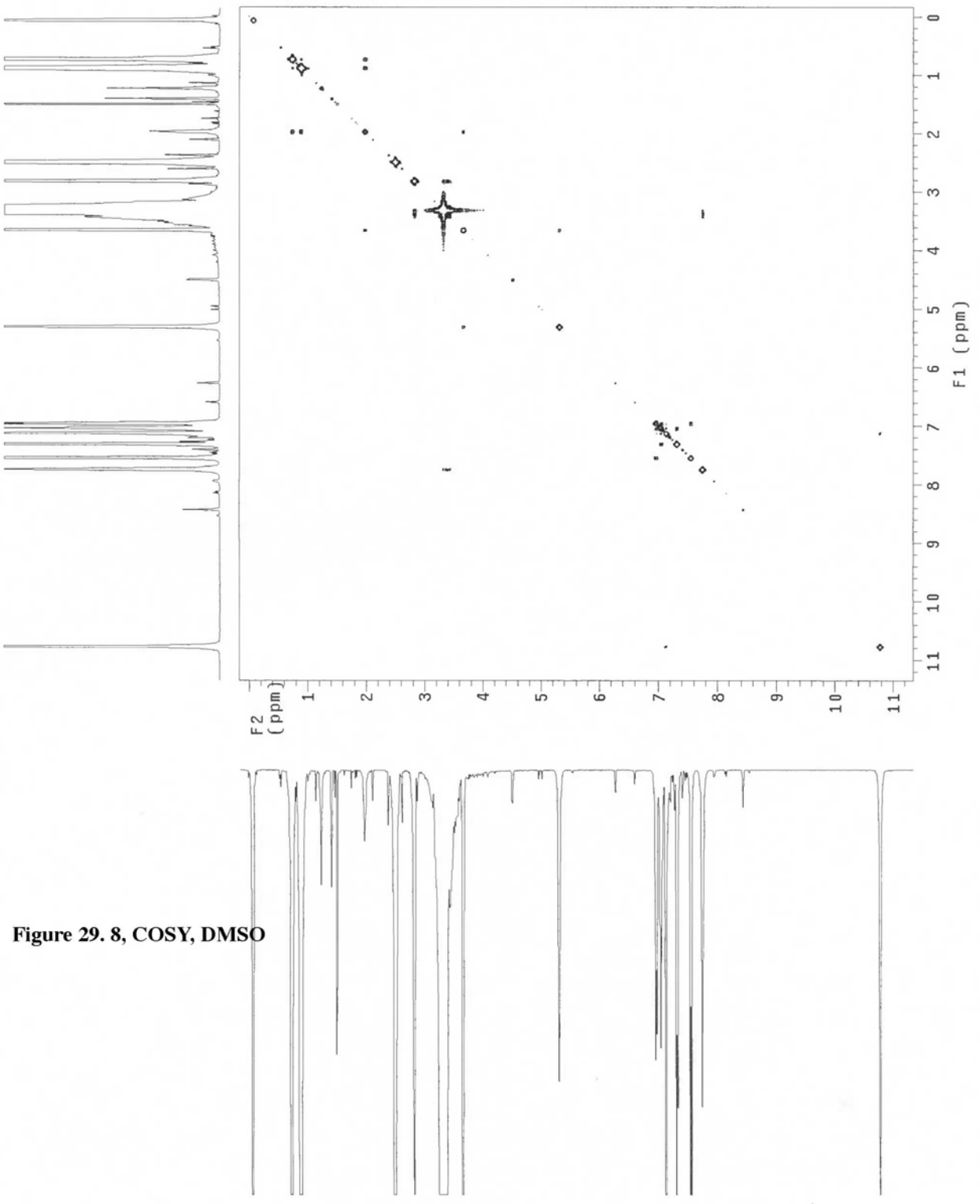

Figure 29. 8, COSY, DMSO

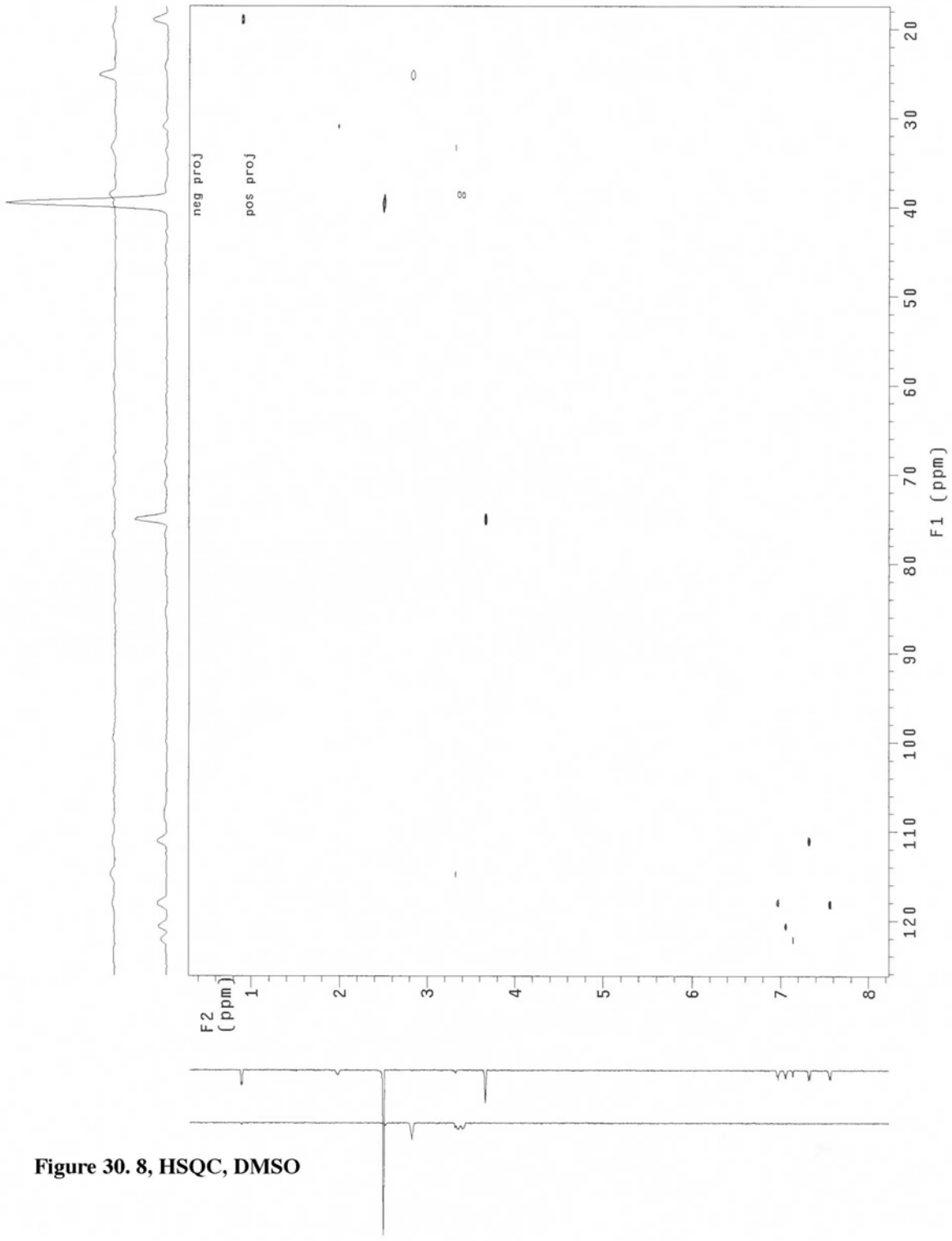

Figure 30. 8, HSQC, DMSO

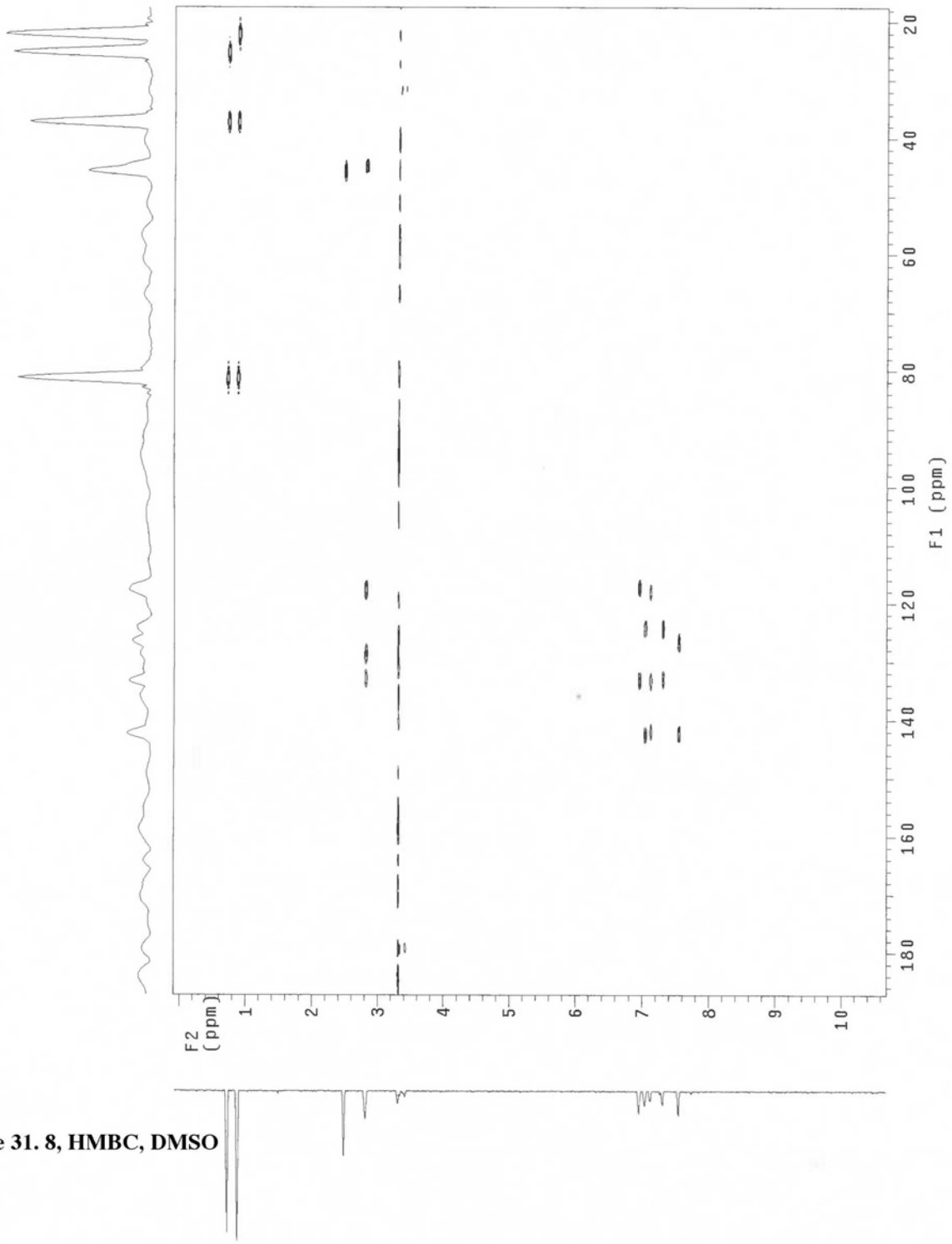

Figure 31. 8, HMBC, DMSO

Supporting Acknowledgements

We thank the University of Illinois mass spectrometry service lab for high-resolution mass determination, and the University of California, Davis, amino acid analysis service lab for individual amino acid concentration determination.

Supporting References

1. Maxwell, P.W., Chen, G., Webster, J.M., and Dunphy, G.B. (1994). Stability and activities of antibiotics produced during infection of the insect *Galleria mellonella* by two isolates of *Xenorhabdus nematophilus*. Appl. Environ. Microbiol. *60*, 715-721.
2. Hu, K., Li, J., and Webster, J.M. (1997). Quantitative analysis of a bacteria-derived antibiotic in nematode-infected insects using HPLC-UV and TLC-UV methods. J. Chromatog. *703*, 177-183.
3. Hu, K., and Webster, J.M. (2000). Antibiotic production in relation to bacterial growth and nematode development in *Photorhabdus--Heterorhabditis* infected *Galleria mellonella* larvae. FEMS Microbiol. Lett. *189*, 219-223.
4. Smigielski, A.J., Akhurst, R.J., and Boemare, N.E. (1994). Phase variation in *Xenorhabdus nematophilus* and *Photorhabdus luminescens*: Differences in respiratory activity and membrane energization. Appl. Environ. Microbiol. *60*, 120-125.
5. Akhurst, R.J. (1980). Morphological and functional dimorphism in *Xenorhabdus spp.*, Bacteria symbiotically associated with the insect pathogenic nematodes *Neoaplectana* and *Heterorhabditis*. J. Gen. Micro. *121*, 303-309.
6. Krasomil-Osterfeld, K.C. (1995). Influence of osmolarity on phase shift in *Photorhabdus luminescens*. Appl. Environ. Microbiol. *61*, 3748-3749.
7. Joyce, S.A., Watson, R.J., and Clarke, D.J. (2006). The regulation of pathogenicity and mutualism in *Photorhabdus*. Curr. Opin. Microbiol. *9*, 127-132.
8. Duchaud, E., Rusniok, C., Frangeul, L., Buchrieser, C., Givaudan, A., Taourit, S., Bocs, S., Boursaux-Eude, C., Chandler, M., Charles, J.F., et al. (2003). The genome sequence of the entomopathogenic bacterium *Photorhabdus luminescens*. Nature Biotech. *21*, 1307-1313.
9. Syn, C.K., and Swarup, S. (2000). A scalable protocol for the isolation of large-sized genomic DNA within an hour from several bacteria. Anal. Biochem. *278*, 86-90.
10. Ho, S., Hunt, H., Horton, R., Pullen, J., and Pease, L. (1989). Site-directed mutagenesis by overlap extesion using the polymerase chain reaction. Gene. *77*, 51-59.
11. Philippe, N., Alcaraz, J.P., Coursange, E., Geiselmann, J., and Schneider, D. (2004). Improvement of pCVD442, a suicide plasmid for gene allele exchange in bacteria. Plasmid. *51*, 246-255.
12. Brachmann, A.O., Joyce, S.A., Jenke-Kodama, H., Schwar, G., Clarke, D.J., and Bode, H.B. (2007). A type II polyketide synthase is responsible for anthraquinone biosynthesis in *Photorhabdus luminescens*. Chembiochem. *8*, 1721-1728.
13. Blodgett, J.A., Thomas, P.M., Li, G., Velasquez, J.E., van der Donk, W.A., Kelleher, N.L., and Metcalf, W.W. (2007). Unusual transformations in the biosynthesis of the antibiotic phosphinothricin tripeptide. Nature Chem. Biol. *3*, 480-485.
14. Sambrook, J., Fritsch, E., and Maniatis, T. (1989). Molecular Cloning: A laboratory Manual, (Cold Spring Harbor Laboratory Press).
15. Richardson, W.H., Schmidt, T.M., and Nealson, K.H. (1988). Identification of an anthraquinone pigment and a hydroxystilbene antibiotic from *Xenorhabdus luminescens*. Appl. Environ. Microbiol. *54*, 1602-1605.
16. Hu, K., Li, J., Li, B., Webster, J.M., and Chen, G. (2006). A novel antimicrobial epoxide isolated from larval *Galleria mellonella* infected by the nematode symbiont, *Photorhabdus luminescens* (Enterobacteriaceae). Bioorg. Med. Chem. *14*, 4677-4681.

17. Li, J., Chen, G., and Webster, J.M. (1997). Nematophin, a novel antimicrobial substance produced by *Xenorhabdus nematophilus* (Enterobactereaceae). Can. J. Microbiol. *43*, 770-773.
18. Li, J., Chen, G., and Webster, J.M. (1996). N-(Indol-3-ylethyl)-2'-hydroxy-3'-methylpentanamide, a novel indole derivative from *Xenorhabdus nematophilus*. J. Nat. Prod. *59*, 1157-1158.
19. Li, J., Chen, G., and Webster, J.M. (1997). Synthesis and antistaphylococcal activity of nematophin and its analogs. Bioorg. Med. Chem. Lett. *7*, 1349-1352.
20. Paik, S., Park, M.K., Jhun, S.H., Park, H.K., Lee, C.S., Cho, B.R., Byun, H.S., Choe, S.B., and Suh, S.I. (2003). Isolation and synthesis of tryptamine derivatives from a symbiotic bacterium *Xenorhabdus nematophilus* PC. Bull. Korean. Chem. Soc. *24*, 623-626.
21. Lang, G., Kalvelage, T., Peters, A., Wiese, J., and Imhoff, J.F. (2008). Linear and cyclic peptides from the entomopathogenic bacterium *Xenorhabdus nematophilus*. J. Nat. Prod. *71*, 1074-1077.
22. Wyatt, G.R. (1961). The biochemistry of insect hemolymph. Annu. Rev. Entomol. *6*, 75-102.
23. Brady, S.F., and Clardy, J. (2005). Cloning and heterologous expression of isocyanide biosynthetic genes from environmental DNA. Angew. Chem. Int. Ed. Engl. *44*, 7063-7065.
24. Brady, S.F., and Clardy, J. (2005). Systematic investigation of the *Escherichia coli* metabolome for the biosynthetic origin of an isocyanide carbon atom. Angew. Chem. Int. Ed. Engl. *44*, 7045-7048.
25. Brady, S.F., Bauer, J.D., Clarke-Pearson, M.F., and Daniels, R. (2007). Natural products from isnA-containing biosynthetic gene clusters recovered from the genomes of cultured and uncultured bacteria. J. Am. Chem. Soc. *129*, 12102-12103.
26. Sleator, R.D., and Hill, C. (2002). Bacterial osmoadaptation: the role of osmolytes in bacterial stress and virulence. FEMS Microbiol. Rev. *26*, 49-71.
27. Burg, M.B., and Ferraris, J.D. (2008). Intracellular organic osmolytes: function and regulation. J. Biol. Chem. *283*, 7309-7313.
28. Culham, D.E., Lasby, B., Marangoni, A.G., Milner, J.L., Steer, B.A., van Nues, R.W., and Wood, J.M. (1993). Isolation and sequencing of *Escherichia coli* gene proP reveals unusual structural features of the osmoregulatory proline/betaine transporter, ProP. J. Mol. Biol. *229*, 268-276.
29. Neidhardt, F.C., Bloch, P.L., and Smith, D.F. (1974). Culture medium for enterobacteria. J. Bact. *119*, 736-747.